1962

An investigation of overlap failures in continuously reinforced concrete pavements. Report No. 7, May 1962

D. Kocaoglu

Continuously Reinforced Concrete Pavements

AN INVESTIGATION OF OVERLAP FAILURES IN CONTINUOUSLY REINFORCED CONCRETE PAVEMENTS

REPORT NO. 7

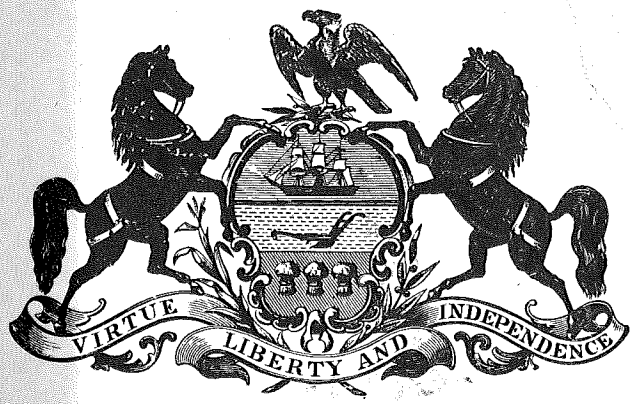

PENNSYLVANIA DEPARTMENT OF HIGHWAYS
AND U. S. DEPARTMENT OF COMMERCE-
BUREAU OF PUBLIC ROADS
IN COOPERATION WITH
LEHIGH UNIVERSITY

CONTINUOUSLY REINFORCED CONCRETE PAVEMENTS

REPORT NO. 7

AN INVESTIGATION OF OVERLAP FAILURES IN CONTINUOUSLY REINFORCED CONCRETE PAVEMENTS

by

Dundar Kocaoglu

Lehigh University

Fritz Laboratory Report 256.12

May 1962

TABLE OF CONTENTS

ACKNOWLEDGEMENTS

This study is a part of the research program on "Continuously Reinforced Highway Pavements" sponsored by the Pennsylvania Department of Highways, The U. S. Department of Commerce - Bureau of Public Roads, and the Institute of Research at Lehigh University.

The work was performed at Fritz Engineering Laboratory, Lehigh University, Bethlehem, Pennsylvania. Professor W. J. Eney is the head of the Department of Civil Engineering and Fritz Engineering Laboratory, Professor L. S. Beedle is the Director of Fritz Engineering Laboratory.

This paper is based upon a thesis which was submitted in partial fulfillment of the requirements for the degree of Master of Science. The author is greatly indebted to Dr. C. L. Hulsbos, thesis supervisor, and Mr. I. J. Taylor, project director, for their continued advice, suggestions and help during the investigation.

SYNOPSIS

Effect of overlaps on the general behavior of continuously reinforced concrete pavements and on the formation of cracks under forces induced by temperature changes was investigated.

Eighteen slab specimens, 22 ft. long with a 12 x 9 inch cross section, were prepared using air entrained concrete with an average 28 day strength of about 4800 psi. The longitudinal reinforcement consisted of two No. 5 bars with a 12 inch overlap at the middle. These specimens were tested under axial forces simulating temperature drops of varying intensities and durations at different ages of the concrete.

The first nine tests were conducted with a static load and all specimens failed at the overlapped region after the formation of uniform crack pattern throughout the entire length. In the second group of tests, dynamic loads simulating daily temperature changes for a period up to one year and more were applied below the ultimate static capacity of specimens. Preformed cracks were induced at the overlap and at two more sections in these specimens and it was observed that the crack at the overlap showed a consistent increase in width while the other cracks had no consistency under repeated temperature changes. These specimens also failed in the vicinity of the ends of

overlaps.

A theoretical study was made for the overlap behavior. Failures were explained by the slip and the loss of bond caused by a crack forming at the lapped section. The theory presented by B. F. Friberg[1] was revised for overlaps and used as the basis of an approach in this analysis.

1. INTRODUCTION

1.1 BACKGROUND

Continuously reinforced highway pavements have been constructed in the last twenty-five years and have shown numerous advantages over conventional highways in this country[3]. Research programs directed by various states have resulted in some criteria concerning the design and construction of continuous pavements. The principal recommendations made as the result of these investigations can be summarized as follows:

1. Steel reinforcement should be between 0.5% and 0.7% (0.5% is the most largely accepted percentage).
2. Thickness of pavement should be about 8".
3. Best location of reinforcement is mid-depth of the pavement.
4. Continuous pavement may be of any length provided that sufficient reinforcement is maintained throughout every section.

The continuously reinforced pavement is permitted to have a series of closely spaced transverse cracks which are controlled to prevent failures from developing. This behavior is accomplished by adequate reinforcement, which usually consists of bar-mats with an overlap at the splices.

Many of the excessive crack openings and eventual failures on continuous pavements in Pennsylvania have been observed to be at the overlapped sections[4]. It has also been noted that highways in Texas, reinforced with individual bars, with random overlaps have shown much better performance than highways constructed with all reinforcement overlapped at a certain transverse section. These observations have indicated the importance of overlaps in continuous pavements and recently more attention has been directed to overlap behavior.

The purpose of this report is to evaluate and discuss the results obtained in laboratory tests performed to investigate the effect of overlaps on general behavior of pavements under temperature variations. Based on the limited number of tests, tentative recommendations for the overlap of reinforcement are also discussed.

1.2 GENERAL PAVEMENT BEHAVIOR

The factors to be considered in design of a continuously reinforced pavement can be discussed in two separate groups as the internal and external forces.

Internal forces are the result of volume changes caused by the shrinkage of concrete and the temperature variations.

Concrete shrinks with loss of moisture. This process takes place in three dimensions and causes axial stresses in the pavement when movement is not permitted. In the longitudinal direction, movement is prevented by the reinforcing steel, and shrinkage results in tension in the concrete. There is no restriction of the contraction of concrete in the transverse direction, and transverse shrinkage constitutes the major portion of total shrinkage. Concrete flows from weaker to stronger sections in the pavement; since the bond is not uniform over the total length, the flow is always toward fully bonded regions causing portions of high tensile stresses in concrete surrounding the reinforcing bar. If these highly stressed portions lie on the same line on adjacent bars, there will be a plane of weakness where cracks can readily form when the tensile stress exceeds the tensile strength of the concrete(5).

Temperature differentials cause volume changes in both the concrete and the steel; and the whole pavement tends to shorten in response to the temperature drops. Since a continuously reinforced pavement is restrained against free contraction by subgrade friction, shortening can not take place and tensile stresses are induced in the slab. If these stresses

exceed the tensile strength of concrete, cracks are formed. A secondary effect of temperature is the formation of warping stresses due to a temperature gradient between the top and the bottom of pavement, but this effect can be superimposed upon previously described tensile stresses.

This report covers the effect of temperature drops which were simulated by applying a tensile force to the test specimens.

Effect of shrinkage of specimens at the time of the tests was negligible compared to the applied temperature drop and was not considered in the calculations.

External forces produced by live loads and subgrade movements were not included in the investigation because the behavior of overlaps was studied in the very early ages of the concrete before live loads would be applied.

2. THEORETICAL ANALYSIS

2.1 INTRODUCTION

An analytical model for the cracked pavement has been proposed by Bengt F. Friberg [1] as shown in Fig. 1. His assumptions are:

1. The steel in the immediate vicinity of the crack is unbonded.
2. Length of the restrained section is sufficient for bond to be fully effective outside the unbonded region.
3. Stress conditions are reversible.
4. Steel and concrete act elastically.
5. Pavement is restrained against movement.

The same basic assumptions will be used in obtaining relationships between crack width, applied load and corresponding temperature drop at the overlapped regions.

Conditions of equilibrium and continuity that were used in Friberg's analysis are:

1. Forces throughout the system must be in equilibrium.
2. Steel and concrete strains are compatible in the section outside the bond-relieved region.

3. Total change in length due to temperature variations is counter-balanced by the steel strains over the total length of the restrained slab (over length "a").

Formation of a crack at a section is accompanied by immediate loss of bond between the steel and the concrete in that vicinity, and stresses are carried only by the steel over the bondless length; so the crack width is a direct measure of total elongation of steel at that section. If the axial stress distribution over the unbonded length of steel is known, the corresponding unit strain and the length of bond-relieved steel can be calculated for every crack width at every section.

Pavement at a cracked section acts the same way as conventional pull-out specimens. Stresses carried only by the steel at a cracked section are transferred into the concrete until equal strains exist in both materials some distance away from the crack. This results in a partially bond-relieved region on both sides of the crack. Bond stresses in this region form stress blocks which are assumed to have distribution patterns similar to the bond-stress blocks in pull-out tests. The transfer of stress from the steel to the concrete takes place until the bond stress at the location exceeds the limiting value and the

bond is lost over a greater length. The ends of the partially unbonded length are similar to the end of steel in pull-out specimens and crack opening in the pavement is comparable to slip at the loaded end of conventional bond tests.

Crack width is equal to the relative elongation and relative movement between concrete and steel in that region. If slip can not take place the full width of the crack corresponds entirely to the summation of strains over a certain length of steel on both sides of the crack. The total length of this unbonded steel is designated with the letter "c".

2.2 NOMENCLATURE

a = Distance between two adjacent cracks

A_c = Concrete area at the section

A_s = Total steel area at the section

b = Length of the bonded region

B = A constant in the equation of a parabola defining the axial stress distribution in steel near a crack

c_1 = Partially bonded length

c_2 = Unbonded length

c = $c_1 + c_2$

c' = Approximate c, neglecting the effect of c_1

c'' = Approximate c, neglecting the effect of c_2

E_c = Modulus of Elasticity of concrete

E_s = Modulus of Elasticity of steel

$f'_{c_{rel}}$ = Relative 28-day strength of concrete in different sets

$\Delta \ell$ = Total change in length of the main test specimens under applied load

p = Steel ratio = A_s/A_c

P = Applied axial load

q = Crack width

ΔT = Temperature drop (°F)

α_c = Coefficient of thermal expansion of concrete

α_s = Coefficient of thermal expansion of steel

α = $\alpha_s = \alpha_c = 6 \times 10^{-6}$ in/in/°F

β = Slip ratio, (Slip/crack width)

ε = Unit strain

ξ = Total slip at the overlap

σ' = Unit stress in the partially bonded steel near a crack

σ_s = Steel stress in bonded region

σ_c = Concrete stress in bonded region

σ' = Stress in completely unbonded steel

2.3 DEVELOPMENT OF EQUATIONS

Relation between Crack Width and Unbonded Length

Crack formation is accompanied by the loss of bond between the two materials resulting in a certain length of steel partially or completely unbonded on both sides of the crack. Relations between the crack width and the corresponding unbonded length are developed below.

a) General

In a restrained slab, crack width is equal to the total elongation of unbonded steel in that vicinity.

$$q = \int_0^c \varepsilon \, ds \qquad \varepsilon = \frac{\sigma}{E_s} \qquad q = \frac{1}{E_s} \int_0^c \sigma \, ds \tag{1}$$

"σ" is a variable over the length c. It reaches its maximum level at completely unbonded sections and is reduced to its minimum value at sections where bond is fully effective. It has been observed in pull-out tests that bond resistance is first developed near the loaded end of the bar and progresses toward portions away from that end. Thus the point of maximum bond stress moves away from the loaded end as the applied load increases. This results in an unbonded portion near the loaded end followed by a partial bond which in turn is followed by a fully bonded region further away from the loaded end[2]. It

will be assumed in our calculations that the axial stress in the steel follows a parabolic distribution in partially bonded regions and its value becomes equal to σ_s, which is practically zero, where bond is fully effective.

b) Sections away from the overlap (No slip).

At a section away from the overlap, crack width is a function of only steel strains since slip can not be expected. Axial stresses on the steel at such a section will be assumed to be distributed as shown in Fig. 2. The crack width can be expressed as:

$$q = \frac{1}{E_s} \int_o^c \sigma \, ds = \frac{1}{E_s} \left[\frac{P}{A_s} \, c_2 + \frac{2}{3} \, \frac{P}{A_s} \, c_1 \right]$$

$$q = \frac{P}{A_s E_s} \left[c_2 + \frac{2}{3} \, c_1 \right] \qquad (2)$$

Eq. (2) can not be directly applied unless more information is available about c_1, the length of partially bonded steel. For practical purposes however, either a constant or a parabolic stress distribution can be assumed over the total length c.

For a constant stress distribution, referring to Fig. 3; crack width is given as

$$q = \frac{P}{A_s E_s} c'$$

Therefore $c' = \frac{q A_s E_s}{P}$ (2a)

in which $c' = \frac{2}{3} c_1 + c_2$

The calculated value for c' is a little less than the actual c.

For a parabolic stress distribution over the total length, as shown in Fig. 4; the crack width becomes

$$q = \frac{2}{3} \frac{P}{A_s E_s} c''$$

$$c'' = \frac{3}{2} \frac{A_s E_s}{P} q \quad (2b)$$

in which $c'' = c_1 + \frac{3}{2} c_2$

The calculated value for c'' is a little higher than the actual c.

Note that Eq. 2a approaches the correct value when the actual c is long and Eq. 2b approaches the correct value for cracks having short c distances. Thus approximation 2a should be used for larger crack openings, 2b for smaller crack openings.

(c) Sections at the overlap (slip present)

As the maximum intensity of bond stress travels nearly the full length of a pull-out specimen, slip takes place between the concrete and the steel. This differential slip does not immediately result in failure because the deformations on the

bar are brought into bearing and a bond resistance is developed by this lug action[2].

Overlaps are comparable to pull-out specimens as explained before. A crack opening at the overlap is therefore partly due to the slip of the unloaded end and partly due to the elongation of unbonded steel as shown in Fig. 5. The equation for crack width is therefore,

$$q = \xi_f + \frac{1}{E_s} \int_o^c \sigma ds$$

or

$$\frac{1}{E_s} \int_o^c \sigma ds = q - \xi_f \qquad (3)$$

The distance "c" is fixed for a crack forming at the end of an overlap because the section should fail as soon as a length equal to overlap loses bond on each side of the crack. Since the overlap length is 12 inches in our test specimens, the fixed c length will always be taken as 24 inches for such cracks.

Final measurements of the crack widths were taken just prior to failure in all specimens. It is assumed that the bond between the steel and the concrete was only due to the lug action at that time. A slip had taken place but the specimen had not failed because of the resistance offered by the deformations on the bar. Failure occurred under a slightly higher load sufficient to overcome the lug resistance. Axial stress

distribution for this condition is assumed to be parabolic for the entire overlap length, the possibility of a completely unbonded region being neglected. This approximation is believed to be justified because of the limited length of the overlap as explained for Eq. 2b. From Fig. 6;

$$q - \xi = \frac{2}{3} \frac{\sigma'_c}{E_s} \qquad (4)$$

substituting $\sigma' = \frac{P}{A_s}$ $\qquad q - \xi = \frac{2}{3} \frac{P}{A_s E_s} c \qquad (4a)$

$$\text{For } c = 24"; \; q - \xi = \frac{16P}{A_s E_s}$$

ξ, slip can be calculated from Eq. 4b as

$$\xi = q - \frac{16P}{A_s E_s}$$

$$\text{For } A_s = 0.62 \text{ in}^2, \; E_s = 30 \times 10^6 \text{ psi}$$

$$\xi = q - 0.86 \times 10^{-3} P \qquad (5)$$

in which q and ξ are in inches and P in kips.

"ξ" could be a function of a number of variables such as the concrete strength, stress in the steel, diameter of the bar, embedment length, and the stress distribution. In the tests performed, the ratio of the calculated ξ to the observed q was computed and was found to be between 50% and 70% in 8 cases out of 10, as shown in Table 19. Based on this observation, it was assumed that ξ, the initial slip is a function of crack width.

$$\xi = \beta q \qquad (6)$$

where β is the ratio $\frac{\text{slip}}{\text{crack width}}$

A value of 60% was used for β for all specimens in further calculations.

The crack near the end of the overlap usually had a considerable width at its formation , from then on it always showed a consistent but slow increase rather than an abrupt change. This behavior can be explained by assuming the initial slip to occur as soon as the crack forms. Therefore, according to this assumption Eq. (6) will always be valid at the overlap since slip will always accompany the crack.

Temperature-Load-Crack relations

Expressions for stresses in the steel and the concrete caused by temperature changes are developed, and the relation between the crack width and the corresponding temperature drop is established below.

(a) General

The condition of equilibrium and continuity are applied as follows:

1. Forces throughout the system are in equilibrium.

$$\sigma_s A_s + \sigma_c A_c = \sigma' A_s$$

$$\sigma_s p A_c + \sigma_c A_c = \sigma' p A_c$$

or $$p\sigma_s + \sigma_c = \sigma' p \qquad (7)$$

where σ_s = Stress in bonded steel.
σ_c = Stress in bonded concrete.
σ' = Stress in completely unbonded steel = P/A_s
p = Steel ratio = A_s/A_c

2. Strains in steel and concrete are compatible in the bonded section.

$$\frac{\sigma_c}{E_c} b - \alpha_c (\Delta T) b = \frac{\sigma_s}{E_s} b - \alpha_s (\Delta T) b \qquad (8)$$

where E_c = Modulus of Elasticity of concrete.
E_s = Modulus of Elasticity of steel.
α_c = Therm. Expansion Coefficient of concrete.
α_s = Therm. Expansion Coefficient of steel.
ΔT = Temperature change.
b = Fully bonded length.

3. The change in length caused by temperature variations is counter balanced by the strains in steel over the length of the restrained slab.

$$\frac{\sigma_s}{E_s} b + \frac{1}{E_s} \int_0^c \sigma \, ds - a (\Delta T) \alpha_s = 0 \qquad (9)$$

where a = length of a restrained portion of the slab, i.e. the average distance between adjacent cracks.

σ = Stress in the partially bonded steel.

On the basis of the assumption that a parabolic axial stress distribution exists on the partially bonded steel, the following relation can be established between σ and σ'.

Referring to Fig. 7;

$$\sigma = \sigma' = P/A_s \qquad (11a)$$

$$\text{for} \quad -\frac{c_2}{2} \leq x \leq +\frac{c_2}{2}$$

$$\sigma = \sigma' - B\,\bar{x}^2 \qquad \text{for} \quad -\frac{c_1}{2} \leq \bar{x} \leq +\frac{c_1}{2}$$

where B is a constant.

$$\sigma = \sigma_s \qquad \text{at } \bar{x} = +\frac{c_1}{2}$$

$$\text{Thus } \sigma_s = \sigma' - B\,\frac{c_1^2}{4}$$

$$\text{Therefore, } B = (\sigma' - \sigma_s)\,\frac{4}{c_1^2}$$

$$B = \left[\frac{P}{A_s} - \sigma_s\right]\frac{4}{c_1^2}$$

$$\text{for } \sigma_s \simeq 0, \; B = \frac{4P}{A_s c_1^2}$$

$$\text{therefore } \sigma = \sigma' - \frac{4P}{A_s c_1^2}\,\bar{x} \quad \text{for} \quad -\frac{c_1}{2} \leq \bar{x} \leq +\frac{c_1}{2} \qquad (11b)$$

Substituting 11a and 11b into Eq. 9 and using the proper limits;

$$\frac{\sigma_s}{E_s}\,b + \frac{\sigma'}{E_s}\left[\frac{2}{3}\,c_1 + c_2\right] - a\,(\Delta T)\,\alpha_s = 0 \qquad (12)$$

Note that the second term in Eq. 12 is equal to q given in Eq. 2 and the discussion for that equation is also valid here. When the total c is short (when the crack is small), c_2 vanishes; when c is long (when crack is large), c_1 becomes negligible.

(b) Sections away from the overlap

For sections away from the overlap, neglecting c_1 in

Eq. 12 and considering $\alpha_c = \alpha_s = \alpha$; the solution of the simultaneous Eqs. 7, 8 and 12 gives:

$$\sigma' = \frac{a\ (\Delta T)\ E_s\ (pn + 1)}{bpn + c\ (pn + 1)} \tag{13}$$

Note: σ' is also equal to P/A_s

$$\sigma_s = \frac{a\ (\Delta T)\ \alpha\ E_s\ pn}{bpn + c\ (pn + 1)} \tag{14}$$

$$\sigma_c = \frac{a\ (\Delta T)\ \alpha\ E_s\ p}{bpn + c\ (pn + 1)} \tag{15}$$

$$\Delta T = \frac{q}{c\alpha} \frac{pn + c/a}{pn + 1} \tag{16}$$

This is the case solved by Friberg[1].

Note that the second approximation for c gives the same result in Eq. 16. If c_2 is considered negligible, the term in brackets in equation 12 is reduced to 2/3 c_1 where c_1 approaches to c'' given by Eq. 2b, making

$$c = \frac{2}{3}\ \frac{3}{2}\ \frac{A_s E_s q}{P} = \frac{A_s E_s\ q}{P}$$

This expression is exactly the same as c' given by Eq. 2a and used as c in Eq. 16.

(c) Sections at the overlap;

Using the same assumption as before, considering the parabolic stress distribution with a value approximately equal

to zero at the unloaded end and a value equal to P/A_s at the loaded end of the overlap, Eq. 12 takes the form

$$\frac{\sigma_s}{E_s} b + \frac{\sigma'}{E_s} \frac{2}{3} c - A (\Delta T) \alpha_s = 0 \qquad (12a)$$

where the second term is identical with $q - \xi$ (Eq. 4)

Solving Eqs. 7, 8 and 12a simultaneously, the following expressions are obtained for cracks at the overlap,

$$\sigma_s = \frac{a (\Delta T) \alpha \, pn \, E_s}{bpn + \frac{2}{3} c (pn+1)} \qquad (17)$$

$$\sigma_c = \frac{a (\Delta T) \alpha \, p \, E_s}{bpn \frac{2}{3} (pn+1)} \qquad (18)$$

$$\sigma' = \frac{a (\Delta T) \alpha E_s (pn+1)}{bpn + \frac{2}{3} c (pn+1)}$$

Since $\sigma' = \frac{3 E_s}{2c} (q - \xi)$ from Eq. 4.

Equating the two expressions for σ' to each other, and substituting $b = a - c$.

$$\Delta T = \frac{3 (q-\xi)}{2c \alpha} \frac{pn + \frac{c}{3a} (2-pn)}{pn + 1} \qquad (20)$$

Using $\xi = 0.6q$ and $c = 24"$ for our specimens, Eq. 20 takes the following form:

$$\Delta T = \frac{q}{40\alpha} \frac{pn + (8/a) (2-pn)}{pn + 1} \qquad (21)$$

The equivalent temperature drop that would have the same effect as the applied load will be calculated for every crack at every load level. Eqs. 16 and 21 will be used for the calculations outside the overlap and at the overlap respectively. Average of ΔT's for all cracks will be taken and referred to as the theoretical value of the temperature drop corresponding to the applied load.

3. TEST PROGRAM

3.1 INTRODUCTION

The specimens were essentially the same as those used in previous research at Lehigh University[6]. Eighteen 22 ft. long specimens were cast with the cross section shown in Fig. 8. In addition to testing these 18 main specimens, auxiliary tests were performed to determine the tensile and compressive strength and the modulus of elasticity of the concrete.

The air temperature in the laboratory was always about 80°F through the test period and the influence of variation of air temperature was neglected in the calculations.

3.2 MATERIALS USED

Hard Grade No. 5 deformed bars made from ASTM A432-59T steel were used as the reinforcement. The average yield strength was about 65,000 psi. No. 3 deformed bars were used as anchors at the end sections of main specimens for gripping the concrete during tensioning operation. No. 2 stirrups were placed around these anchor bars in order to reduce the probability of undesirable cracks at the ends. Physical properties of the steel are shown in Table 1.

Six pours of concrete were made, each pour being sufficient for three specimens. The twenty eight day compressive strength of the batches varied between 3700 and 5400 psi.

Ready-mix concrete was used which had a 620:1070:1940 by weight mix, with an air entrained cement. Water was added in the laboratory in amounts varying between 20 and 25 gallons per cubic yard of concrete, depending on the moisture content of aggregate and sand, which resulted in slumps from 1 3/4 to 4 inches. The maximum size of the course aggregate was 1 inch.

3.3 MAIN TESTS

Specimens 22 ft. long, 9 1/2 inches thick and 12 inches wide were poured on a 1/2 inch thick rubber mat resting on 3/4 inch plywood forms. A sheet of tarred paper was placed between the rubber mat and the concrete for the purpose of reducing base friction to a minimum. The concrete was placed and exposed to the air with no special curing employed.

Reinforcement consisted of two No. 5 deformed bars at mid-height providing a steel ratio of 0.54%. Length of the end anchors varied between 12 to 18 inches with stirrups placed at 4 inch intervals. At the fixed end of specimens; the

reinforcing bars and the end anchors were connected to a channel fastened to the floor by two 3 inch diameter round studs. At the moving end, the fixed channel bore against mechanical jacks which, in turn, rested against a movable channel. Five one inch round rods were used for connecting the ends of each specimen to the channels.

Dynamometers were placed at both ends of the specimens for measuring the total tensile force applied. Figs. 9 and 10 show the fixed and moving ends respectively. Fig. 11 is a close-up of dynamometers. Total length change was measured at every load increase in each test. In the first three specimens, this was done by stretching an invar wire between the two ends and measuring the movement of its end with the use of a dial gage placed on the fixed end side of the wire; in the other specimens a dial gage was placed at each end and their differences were taken at every load interval. These end gages rested against a small plate welded to a 4 inches high bar embedded in the concrete about 6 inches from the end of specimen. The dial gage is shown in Fig. 12.

Reinforcing bars were placed into the forms with a 12 inch overlap at the middle as shown in Fig. 13. They were bolted to the end fixtures of each specimen on both ends.

Overlaps always extended 6 inches to both sides of the mid-section. Fig. 14 shows the general test set-up.

Crack widths were measured with an optical device (Fig. 15) and an average width was obtained from 3 to 5 readings taken on the top and two sides at each crack. In the last six specimens, a Whittemore gage was also used at three sections (Fig. 16). A fairly uniform crack pattern was observed over the entire length. Within three feet of the ends, cracks usually formed at the bottom of the specimen, but did not reach the top. These cracks were believed to be caused by end fixture effects and were disregarded.

The specimens were given numbers from I to XVIII and grouped in six sets designated with letters from A to F.

The first twelve specimens, I to XII, were loaded separately with static tensile forces applied to the moving end by 50-ton capacity jacks. For loading the middle specimen, both jacks were used simultaneously at the same loading rate. The connecting rods on the other two specimens were loosened to prevent them from being loaded. For loading a side specimen the near jack was used, a 1 inch round bar was placed as a fulcrum near the opposite jack and again the connecting rods of the other two specimens were loosened.

Specimens I to IX (Sets A to C) were loaded until failure. At every crack formation during the course of the test; loading was stopped, total load, total change in length and the widths and locations of all cracks were measured.

In Set D; P_{cr}, the load at which the first crack would form, was calculated for different ages of concrete, and specimens X, XI, XII were loaded with $0.3P_{cr}$, $0.5P_{cr}$, $0.7P_{cr}$ respectively. Loading was started when the age of concrete was 8 hours and was continued for 28 hours at 4 hour intervals. After the age of concrete was 36 hours, a continuous load was applied to each specimen up to failure. Crack, load and length measurements were taken the same way as was done in sets A, B, C.

In specimens XIII to XVIII (Sets, E,F) three sections were intentionally made weaker (midpoint and 5 ft. from each end in Set E, end of overlap and 5 ft. from each end in Set F) by inserting a metal plate at those sections before the concrete was poured. Specimens were loaded statically until the cracks were formed at the weakened sections and then a dynamic load was applied by means of a hydraulic jack and a timing device which regulated loading and unloading time. Fig. 17 shows the load control unit and the timer. A complete cycle of loading

and unloading took four minutes. Variation of the load was recorded using a static strain indicator, an amplifier and a strip chart recorder as shown in Fig. 18.

Specimen XIII failed as soon as the dynamic loading was started. Specimen XIV was subjected to the cracking load for 200 cycles, then the load was increased up to failure. Cracking load was applied to specimen XV for 30 cycles, then it was increased to a level a little lower than P_{ult}, where P_{ult} is the load which would cause failure if applied statically. After applying the new load 9 cycles, the specimen failed.

Specimen XVI was subjected to a load equal to 75% of P_{ult}. After 22 cycles under that load, two cracks were formed in addition to three preformed cracks. When the test was stopped at the end of 365 cycles, the specimen was very near the point of failure. It was completely failed later under a slightly higher load.

Specimen XVII was loaded at 84.4% of P_{ult} for 2881 cycles. Load was then increased to a level slightly below the ultimate and failure was obtained at the end of 14 cycles under the new load.

Specimen XVIII was subjected to 94% of P_{ult} and failed at the end of 251 cycles.

Crack widths were measured at 4 to 5 hour intervals in all dynamic tests. Cracks at the mid-section showed a consistent increase through the course of the test while the other cracks had an inconsistent change (sometimes increasing, sometimes decreasing). Failure was always at the end of the overlapped region.

Test data are presented in Tables 3 to 18. Figs. 19 to 24 show the crack pattern and failure details after the tests were completed.

3.4 AUXILIARY TESTS

(a) Tension tests on concrete.

Direct information on the tensile strength of concrete is not readily available because of its very limited use. However, it is important in continuously reinforced highway pavements because the amount of steel required is determined from the concrete tensile strength. A higher steel percentage is needed as the tensile strength of concrete is increased.

Two tension specimens were tested for every batch of concrete after the specimens were exposed to air for 7 days.

The test set up was prepared as shown in Fig. 25. A

46 x 20 x 3/4 inch plywood base plate resting on five 3/4 inch thick supports was placed between two stud columns which were fixed to floor by means of 3 inch round studs. Test specimens 44 inches long, 10 x 6 inches in area with a reduced cross section of 6 x 6 inches at the middle, were poured on a 1/2 inch thick rubber mat. A layer of tarred paper was placed between the concrete and the rubber mat to reduce base friction as much as possible.

A threaded one inch round steel rod was placed into the concrete at both ends of each specimen at mid-height. One of the bars was fixed at the stud column. A tubular dynamometer and a hydraulic jack were placed on the other bar for loading the specimen.

A manually operated hydraulic jack was used for the application of the load which was measured by indicators connected to the SR-4 gages on the dynamometer. Figs. 26 and 27 show tension tests. Failure was always at the reduced cross section as shown in Fig. 27.

(b) Compression tests on concrete

Standard 6 x 12 inch cylinders were used in compression tests. Fifteen cylinders were prepared for each set; 3 of them were cured in moist room for 28 days and modulus of elasticity

tests were performed at the end of that period. Three cylinders were tested after being exposed to air for 7 days to obtain the 7-day compressive strength corresponding to the tensile strength obtained from tension tests performed at the same time. The remaining 9 cylinders were air dried and tested for compressive strength and modulus of elasticity of the concrete at the time of the failure of the main specimens.

Results of all auxiliary tests are shown in Table 2.

4. TEST RESULTS

Concrete properties shown in Table 2 were obtained from the auxiliary tests performed on the 7th and 28th days after the test specimens were cast. Each figure is the average of 2 or 3 tests. The relative concrete strength, $f'_{c_{rel}}$ given in the last column is an index for comparing relative strength of concrete used in each set.

Data taken during the main tests are presented in Tables 3-18. The sketch at the top of each table shows the sequence of the cracks that extended to the top of the slab prior to failure. Widths of the cracks under various loads are shown in tabular form. Temperature given under each load is the corresponding temperature drop that would have caused the same effect as the applied axial load as calculated from data by the formulas developed in chapter 2.

Temperature drop corresponding to each load was also calculated from the total length change in specimens. Difference between the readings of dial gages on the two ends indicated the total change in the length of the specimen at every load level. Average strain in the specimen was calculated from this length change and the strain was converted into the corresponding

temperature drop, assuming a coefficient of thermal expansion equal to 6×10^{-6}in/in/°F for the specimen. In table 20, these temperature changes were listed together with the ΔT values calculated from the equations developed in Chapter 2. In specimens II, III, XIII, XV and XVII; the total length change could not be measured and the corresponding temperature drop could not be computed.

The data from Table 20 are plotted in Figs. 28 to 30 to show the relation of age of pavement to the temperature drop to cause failure. These graphs also compare the two methods for finding ΔT. As seen in all cases the two values for ΔT are reasonably close to each other. Figs. 28 and 30 show the effect of time on the failure of pavements. The general trend under all loading conditions was that in the early age of the concrete a relatively low temperature was sufficient to cause failure.

If failure did not occur at overlap during a critical period in the beginning, then overlap became less critical for the remaining life of the specimens. The critical time was about 5 days in our dynamic tests. The graph in Fig. 30 has a steep slope up to the point where the age of concrete is 4 - 5 days; from then on it has a very smooth curve, almost

a constant temperature. Practically the same temperature drop was required for the failure of a specimen at the end of 14 days as another specimen in about 5 days.

Width of the crack at the overlap increased continuously until failure in specimens less than 5 days old. In specimen XVII, however, the increase stopped twice and restarted after a short time. Each time, the width of the crack at the overlap attained more or less the same limiting value and did not increase any further. This is an indication that the most critical time for the overlaps is the early days of pavement life. As the concrete gains its maximum strength overlaps act similar to other sections.

Fig. 31 presents a comparison of different loading conditions. The effect of differences in the concrete quality of specimens was eliminated by introducing the index $f'_{c\,rel}$ into the curves.

The curve representing dynamic loading is more or less parallel to the static loading curve with a difference of about 1 1/2 days at every load level. The graph indicates that a pavement under the influence of a large number of temperature variations will fail at the overlap, at a much lower temperature

difference than a pavement subjected to a small number of variations at the same age. A significant point is that the curve for Set D is between the static and dynamic test curves. A combination of static and dynamic loads was used in testing Set D specimens and even a small amount of dynamic loading has shown its effect by placing the curve in between the other two cases.

In Tables 16 to 18, the calculated temperature drops are also listed at various cycles under repeated load with a constant maximum value for specimens XVI, XVII and XVIII. The results show that a repeated constant stress produces the equivalent effect on the general pavement behavior as an increasing temperature differential. Total length changes rather than the stresses are involved in the evaluation of temperature variations. In the laboratory tests, a constant stress does not correspond to a constant temperature change, but a constant change in the length always represents a constant temperature differential.

In the actual pavements, a temperature change causing high stresses in the beginning would result in lower stresses later. This is due to the bondless region getting longer after each crack formation. The change in length due to temperature differentials will be counter-balanced by strains over a greater

length, requiring lower unit strains, and in turn, causing lower stresses as the pavement gets older.

The data showing the effect of cycling on the corresponding temperature drop were plotted in Figs. 32 and 33 respectively.

5. CONCLUSIONS

Interpretation of results is limited by the few tests performed, but the general conclusions drawn from the investigation can be summarized as follows:

1. Initial random cracks are distributed fairly uniform over the total length of pavement. They have a tendency to form at about equal intervals, and they may also form at the ends of the overlapped regions.

2. A crack at the overlap is likely to develop into failure while cracks at other sections are not apt to cause the pavement to fail. Therefore, the ends of the overlaps constitute weak sections in continuously reinforced pavements.

3. Mechanism of failure is by the loss of bond at cracked section. As soon as a crack forms, bond between steel and concrete is lost over a certain distance on both sides of the crack. This bondless section could be quite long without causing failure at sections outside the overlaps, but if the crack is near the overlap and if the bondless section extends over the entire length of overlap, then failure is immediate.

4. Overlap failures are originated in the early ages of pavement. If a crack does not occur at the overlap during the first 4-5 days, it is not as likely that the failure will

ever occur. After the initial critical period of time, overlaps act similar to the other sections.

5. A pavement subjected to mild but frequent temperature variations is more likely to fail than a pavement under the action of seldom but more severe temperature variations.

6. In order to be able to predict crack widths and failures the yield point of the steel should not be exceeded.

7. The axial stresses caused by a temperature change are higher in the early ages of the pavement in comparison with the stresses caused by the same change at a later age.

8. The following two methods are suggested for the elimination of overlap failures:

a) Increasing the overlap lengths, so that greater temperature variations will be necessary to relieve the bond over that length.

b) Placing overlaps at random, rather than at the same section. This will eliminate the cumulative weakening effect of all overlaps at a section the most likely to fail.

Further investigation is necessary to obtain more quantitative results and to make rational design suggestions concerning the overlaps. The following subjects need to be

given special study under static and repeated loads:

1. Formation and distribution of bond stresses at overlaps.

2. Effect of random spacing of overlaps and increased length at overlaps. This study will help to make design methods more effective and will prove or disprove the suggestions listed as item 8 in Conclusions.

3. An investigation for steel stresses exceeding the yield point. This might give valuable information about the exact behavior of overlaps which can not be predicted beyond the yield level of steel with the available methods.

4. Bond-slip relations at overlaps.

6. TABLES

TABLE 1 - PHYSICAL PROPERTIES OF STEEL BARS

Bar Designation	Used in Specimens	Yield Strength (psi)	Tensile Strength (psi)
No. 5	I to III	62500	115,000
No. 5	IV to XII	65000	105,900
No. 5	XIII to XVIII	65300	106,300
No. 3	I to VI	80000	137,600
No. 3	VII to XVIII	76900	113,000

TABLE 2 - PROPERTIES OF CONCRETE

Set	Specimens	f_t'-psi (7-day)	f_c' - psi		E_c - 10^6 psi 28 day	Slump (in)	*Relative f_c' 28-day
			7-day	28-day			
A	I-III	378	3490	5054	3.92	1 3/4	1.36
B	IV-VI	167	3553	4780	3.84	3 1/4	1.28
C	VII-IX	228	3667	4333	3.63	2 1/2	1.16
D	X-XII	283	4033	5728	4.18	2 1/8	1.54
E	XIII-XV	265	3025	3722	4.45	4	1.00
F	XVI-XVIII	394	4623	5400	3.97	2 1/2	1.45
Average		286	3732	4836	4.00		

* Based on the 28-day f_c' of Set E.

TABLE 3 - CRACK WIDTHS* - SPECIMEN I

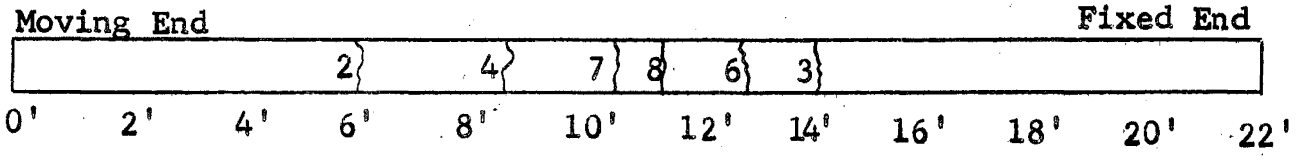

Location of Cracks

P-kips		22.3	24.25	24.25	25.8	27.8
ΔT-°F		28.4	35.7	52.1	64.3	77.7
Crack Number	2	14	14	14	14	14
	3		10	10	10	10
	4			16	16	16
	6				16	16
	7					28
	8					4

* Crack widths in 10^{-3} inches

P = Applied tensile load

ΔT = Calculated temperature change to produce the same effect as the applied load.

TABLE 4 - CRACK WIDTHS* - SPECIMEN II

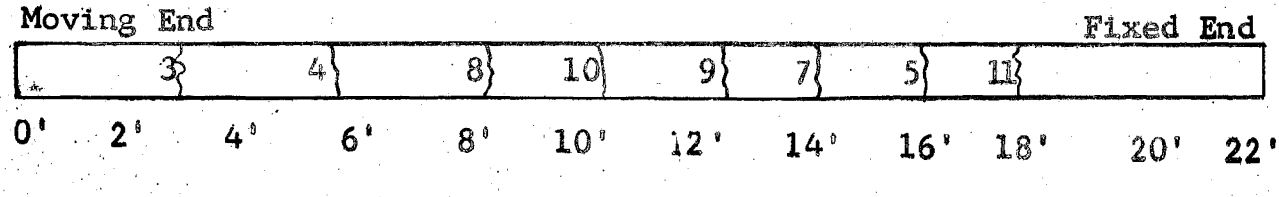

Location of Cracks

P-kips		21.2	21.7	24.5	24.8	28.1	29.4	30.7
ΔT-°F		26.6	32	58.8	94	121	128.1	147.6
Crack Number	3			12	22	22	22	22
	4	9	16	16	25	25	25	25
	5		9	19	22	22	22	24
	7			12	20	22	22	22
	8				15	25	25	35
	9					24	24	25
	10						20	25
	11							15

* Crack widths in 10^{-3} inches

P = Applied tensile load

ΔT = Calculated temperature change to produce the same effect as the applied load.

TABLE 5 - CRACK WIDTHS* - SPECIMEN III

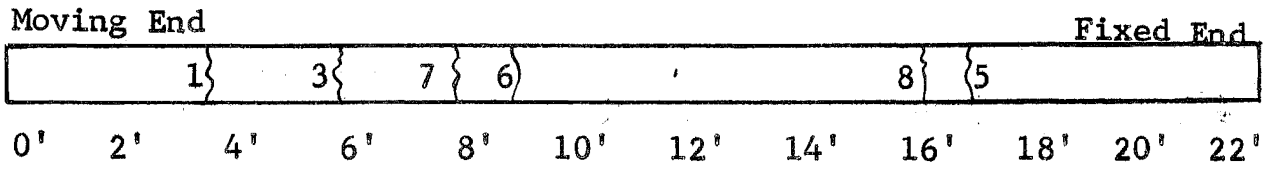

Location of Cracks

P-kips		25.5	30.8
ΔT-°F		33.6	169.9
Crack Number	1		35
	3	18	33
	5		25
	6		45
	7		50
	8		35

* Crack widths in 10^{-3} inches

P = Applied tensile load

ΔT= Calculated temperature change to produce the same effect as the applied load.

TABLE 6 - CRACK WIDTHS* - SPECIMEN IV

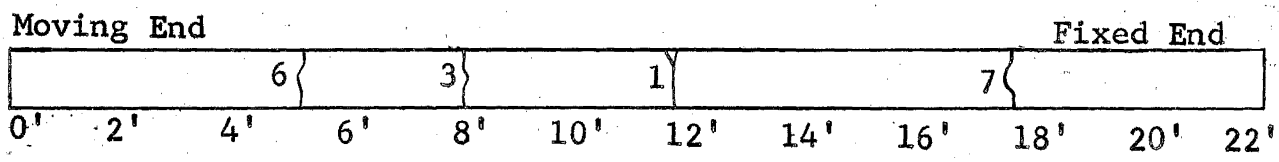

Location of Cracks

P-kips		7.5	8.7	9.5
ΔT-°F		22.5	29	29.8
Crack Number	1	17	21	24
	3	10	10	10
	6		5	5
	7		6	6

*Crack widths in 10^{-3} inches

P = Applied tensile load

ΔT = Calculated temperature change to produce the same effect as the applied load.

TABLE 7 - CRACK WIDTHS* - SPECIMEN V

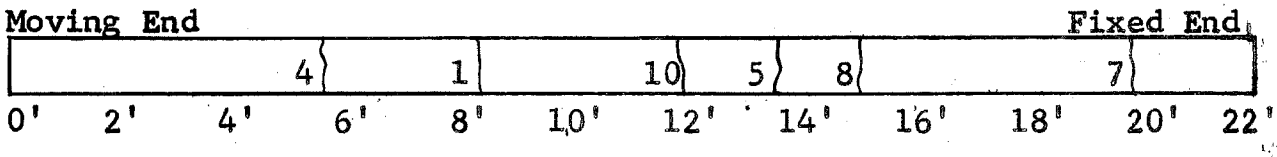

Location of Cracks

P-kips		8	10.5	12.3	14.3
ΔT-°F		13.5	31.2	61.6	86.1
Crack Number	1	5	11	20	20
	4		10	15	15
	5			23	23
	7			5	5
	8			10	10
	10				14

* Crack widths in 10^{-3} inches

P = Applied tensile load

ΔT = Calculated temperature change to produce the same effect as the applied load

TABLE 8 - CRACK WIDTHS* - SPECIMEN VI

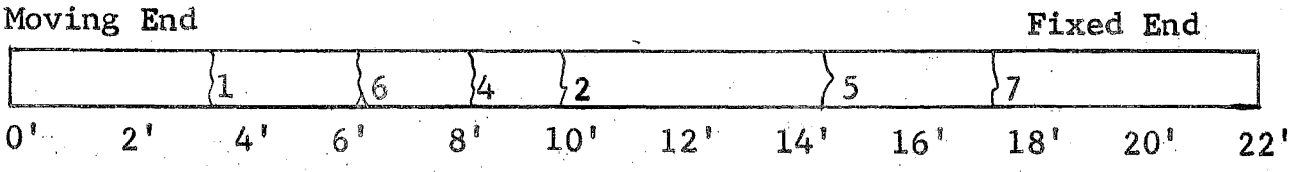

Location of Cracks

P-kips		15	17	19.3	20	20.2	21.6	23.5
ΔT-°F		12.5	21.4	53.6	56.8	68.5	80.5	79.7
Crack Number	1	3	3	8	8	8	20	20
	2		10	18	18	18	18	18
	4			8	8	8	8	8
	5			12	12	12	12	12
	6				12	12	15	23
	7					15	15	15

* Crack widths in 10^{-3} inches

P = Applied tensile load

ΔT = Calculated temperature change to produce the same effect as the applied load

TABLE 9 - CRACK WIDTHS* - SPECIMEN VII

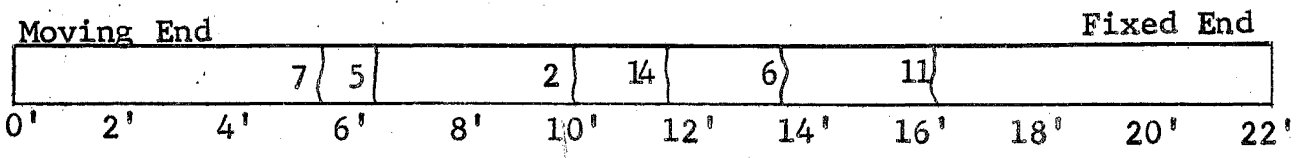

Location of Cracks

P-kips		9.8	9.9	11.1	13.4
ΔT-°F		22.7	24.6	35.2	56.2
Crack Number	2	14	14	14	23
	5		5	5	10
	6			9	14
	7			8	13
	11				10
	14				4

* Crack widths in 10^{-3} inches

P = Applied tensile load

ΔT = Calculated temperature change to produce the same effect as the applied load.

TABLE 10 - CRACK WIDTHS* - SPECIMEN VIII

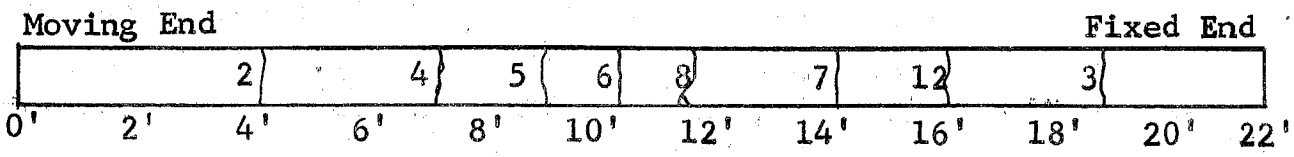

Location of Cracks

P-kips		11.7	11.9	12	13.1	13.5	15.7	16	16.3
ΔT-°F		13.6	22.6	39.7	45.7	54.6	74.6	77.7	85.3
Crack Number	2	6	6	6	6	6	6	6	6
	3	2	2	2	2	2	2	2	2
	4		11	11	11	13	13	13	13
	5			13	20	25	25	25	25
	6						12	12	20
	7				10	10	10	10	10
	8					5	5	5	10
	12							17	22

*Crack widths in 10^{-3} inches

P = Applied tensile load

ΔT = Calculated temperature change to produce the same effect as the applied load.

TABLE 11 - CRACK WIDTHS* - SPECIMEN IX

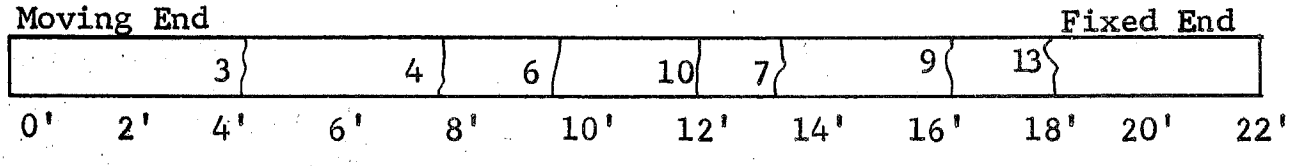

Location of Cracks

P-kips		15	16.4	18.1	18.7
ΔT-°F		41.1	77.7	91.3	98.3
Crack Number	3	11	11	11	11
	4	20	20	20	20
	6	3	3	3	3
	7	23	23	28	28
	9		13	15	15
	10		10	23	32
	13				11

* Crack widths in 10^{-3} inches

P = Applied tensile load

ΔT = Calculated temperature change to produce the same effect as the applied load.

TABLE 12 - CRACK WIDTHS* - SPECIMEN X

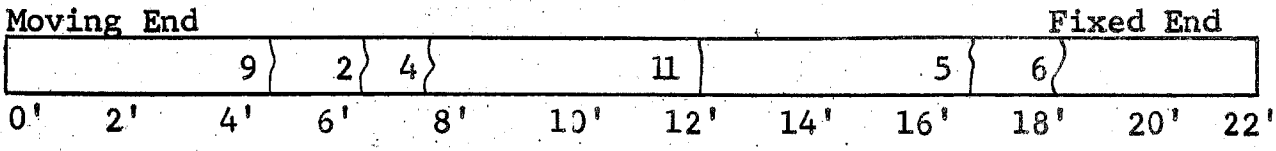

Location of Cracks

P-kips		26	26.3	26.6	28.3	30.8
ΔT-°F		46.8	72.2	72.4	72.6	156.5
Crack Number	2	20	30	30	30	41
	4		6	6	6	28
	5		14	32	32	45
	6					7
	9				11	18
	11					70

* Crack widths in 10^{-3} inches

P = Applied tensile load

ΔT = Calculated temperature change to produce the same effect as the applied load.

TABLE 13 - CRACK WIDTHS* - SPECIMEN XI

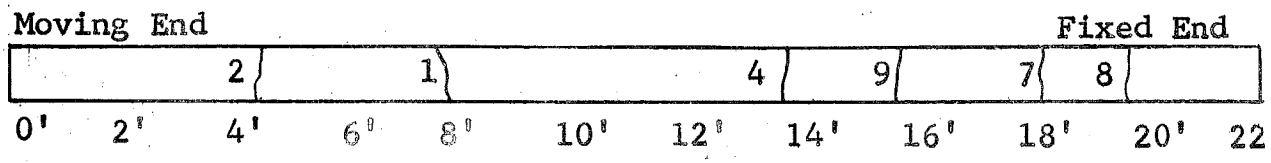

Location of Cracks

P-kips		31.5	31.7	32.6	35	35.1	36.4
ΔT-°F		59.8	81.7	158.4	145	156.8	169.5
Crack Number	1	20	30	50	50	50	50
	2	12	20	25	25	25	25
	4		10	44	44	44	50
	7				25	25	25
	8				5	5	12
	9					13	13

* Crack widths in 10^{-3} inches

P = Applied tensile load

ΔT = Calculated temperature change to produce the same effect as the applied load.

TABLE 14 - CRACK WIDTHS* - SPECIMEN XII

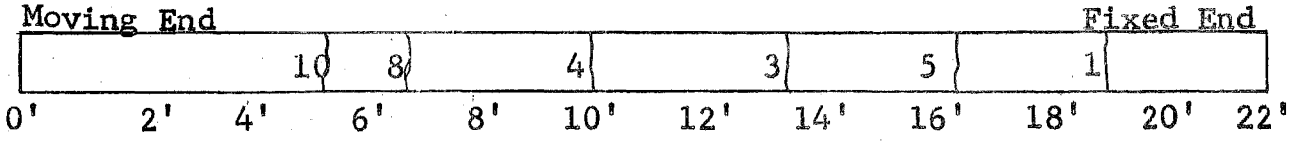

Location of Cracks

P-kips		26.6	27.2	33.5	33.9
ΔT-°F		61.4	72.7	111.2	153.4
Crack Number	1			15	15
	3	40	55	90	90
	4			30	95
	5		10	10	10
	8			40	45
	10				10

* Crack widths in 10^{-3} inches

P = Applied tensile load

ΔT = Calculated temperature change to produce the same effect as the applied load.

TABLE 15 - CRACK WIDTHS* - SPECIMENS XIV AND XV

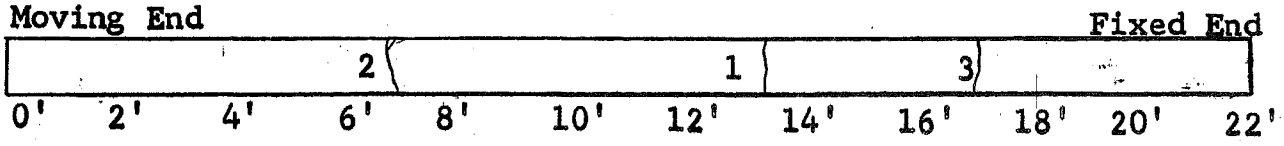

Location of Cracks - Specimen XIV

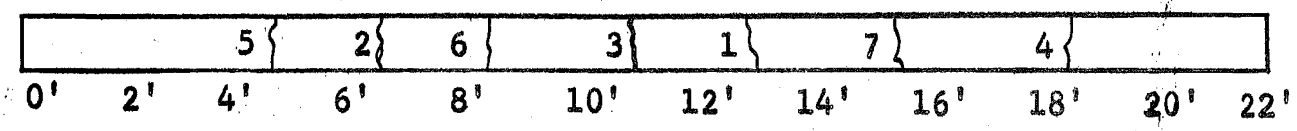

Location of Cracks - Specimen XV

SPECIMEN XIV

P-kips		15	15
Age-Hrs.		33	47
ΔT-°F		53.4	53.8
Crack No.	1	19	16
	2	18	18
	3	18	21

SPECIMEN XV

P-kips		25
Age-Hrs		53
T-°F		92.9
Crack Number	1	15
	2	20
	3	5
	4	5
	5	5
	6	10
	7	30

* Crack widths in 10^{-3} inches

P = Applied tensile load

ΔT = Calculated temperature change to produce the same effect as the applied load.

TABLE 16 - CRACK WIDTHS* - SPECIMEN XVI

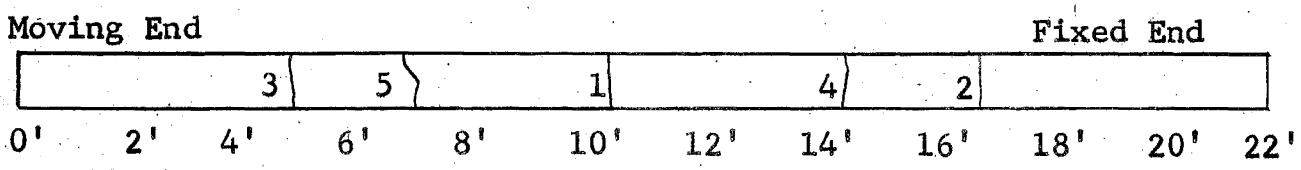

Location of Cracks

P-kips		24	24	24	24	24	24
Cycles		1	22	140	306	350	365
Age Hrs		46	48	55	66	69	70
ΔT-°F		43.8	98.5	122.1	116	120.5	130.2
Crack Number	1	25	25	32	41	45	50
	2	5	7	9	10	8	8
	3	25	25	35	43	40	44
	4		33	45	46	47	49
	5		34	35	20	24	28

* Crack widths in 10^{-3} inches

P = Applied tensile load

ΔT = Calculated temperature change to produce the same effect as the applied load.

TABLE 17 - CRACK WIDTHS* - SPECIMEN XVII

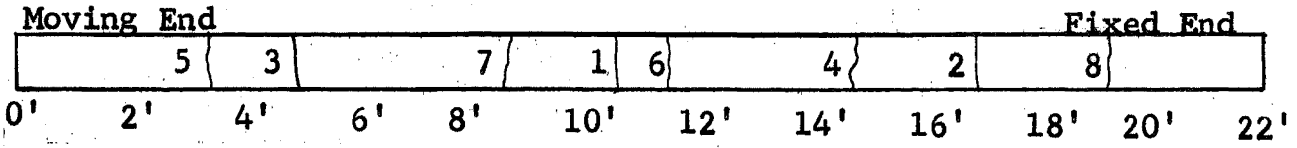

Location of Cracks

P-kips		27	27	27	27	27	27	27	27
Cycles		1	68	121	230	323	365	365	460
Age-Hrs		73	78	82	90	97	100	167	174
ΔT-°F		68.8	68.9	91.9	96.5	96.5	100.1	91.2	92.2
Crack Number	1	23	30	33	33	35	35	27	30
	2	9	12	18	20	20	25	23	20
	3	31	32	38	40	40	35	38	38
	4	30	30	39	41	40	40	35	38

P-kips		27	27	27	27	27	27	27	27
Cycles		641	676	722	805	995	1138	1345	1419
Age-Hrs		186	189	192	198	211	221	235	240
ΔT-°F		92.4	96.2	97.8	103.9	110.5	124.9	137	125.2
Crack Number	1	36	37	40	40	45	48	49	49
	2	20	23	20	20	23	20	23	20
	3	40	35	36	35	40	40	39	40
	4	35	40	40	50	50	44	50	50
	5						30	35	25

TABLE 17 continued.

P-kips		27	27	27	27	35
Cycles		2247	2879	2879	2881	2895
Age-Hrs		291	308	332	335	336
ΔT-°F		136.4	142.6	130.7	117.7	153
Crack Number	1	49	50	45	45	16
	2	21	25	20	25	30
	3	40	43	41	40	48
	4	50	50	50	45	45
	5	35	36	30	15	40
	6					70
	7					15
	8					30

* Crack widths in 10^{-3} inches

P = Applied tensile load

Δ T = Calculated temperature change to produce the same effect as the applied load

TABLE 18 - CRACK WIDTHS* - SPECIMEN XVIII

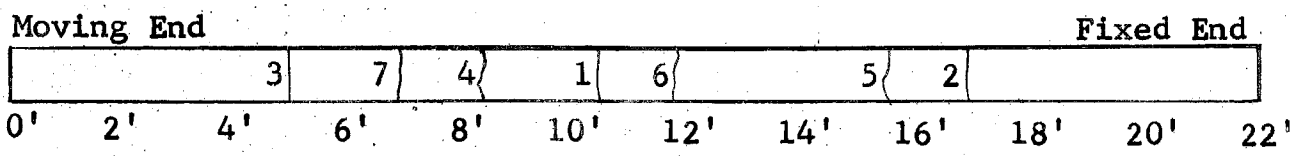

Location of Cracks

P-kips		30	30
Cycles		1	251
Age-Hrs		101	107
ΔT-°F		109.1	145
Crack Number	1	10	2
	2	3	28
	3	50	60
	4	50	21
	5	22	20
	6		70
	7		25

* Crack widths in 10^{-3} inches

P = Applied tensile load

ΔT = Calculated temperature change to produce the same effect as the applied load.

TABLE 19 - "β" SLIP RATIO

Specimen	"q" at overlap (10^{-3} in)	P (Kips)	$\frac{2}{3}\frac{P}{A_s E_s}c$ (10^{-3} in)	$\xi = P - \frac{2}{3}\frac{P}{A_s E_s}c$ (10^{-3} in)	$\beta = \frac{\xi}{q} \times 100$
I	32	27.8	23.9	8.1	25.3
II	25	30.7	25.4	-0.4	
III	45	30.8	25.5	19.5	43.3%
IV	24	9.5	8.2	15.8	65.9%
V	-				
VI	-				
VII	27	13.4	11.5	15.5	57.3%
VIII	30	16.3	14	16	53.3%
IX	-				
X	70	30.8	25.5	44.5	63.6%
XI	-				
XII	95	33.9	29.1	65.9	69.4%
XIII	-				
XIV	-				
XV	-				
XVI	50	24	20.6	29.4	58.8%
XVII	86	35	30.1	55.9	65.0%
XVIII	72	30	25.8	46.2	64.1%

Note: c = 24", A_s = 0.62 in^2. E_s = 30 x 10^6 psi were used.

TABLE 20 - CORRESPONDING TEMPERATURE DROPS IMMEDIATELY BEFORE FAILURE OF SPECIMENS

Specimen	Age of Concrete - Hrs		ΔT from $\Delta \ell$	Theoretical ΔT	$\frac{\Delta T_{theory}}{f'_{c_{rel}}}$
	Beginning of test	Prior to Failure			
I	20 hours	21 hours	61°F	77.7°F	57.2
II	30 hours	31.5 hrs	-	147.6°F	108.5
III	40 hours	41 hours	-	169.9°F	125
IV	8 hours	9 hours	30°F	29.8°F	23.2
V	12 hours	13 hours	83°F	86.1°F	48.2
VI	16 hours	17 hours	78°F	79.7°F	62.3
VII	8 hours	8.5 hrs	49°F	56.2°F	48.5
VIII	10 hours	11 hours	79.5°F	85.3°F	73.7
IX	12 hours	13 hours	91°F	98.3°F	84.8
X	8 hours	37.5 hrs	131°F	156.5°F	102
XI	8 hours	40 hours	145°F	169.5°F	110
XII	8 hours	39.5 hrs	155°F	153.4°F	99.5
XIII	24 hours	25 hours	-	-	-
XIV	26 hours	47 hours	55°F	53.8°F	53.8
XV	50 hours	53 hours	-	92.9°F	92.9
XVI	46 hours	70 hours	135°F	130.2°F	89.9
XVII	73 hours	14 days	-	153°F	105.7
XVIII	101 hours	109 hours	149°F	145°F	100

7. FIGURES

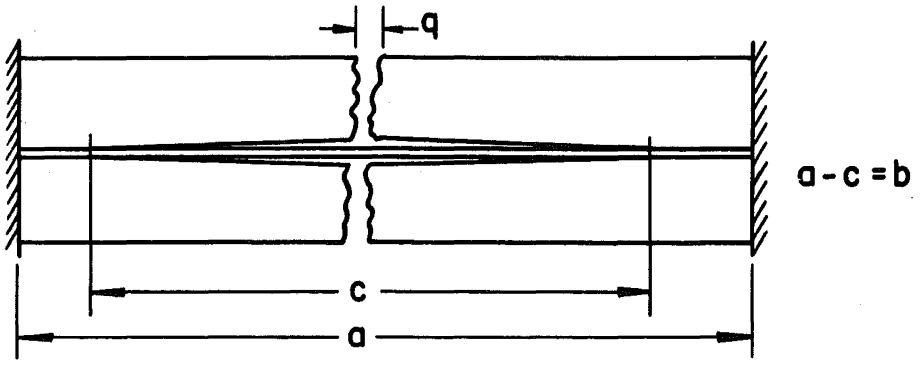

FIG. 1 FULLY RESTRAINED CRACKED PAVEMENT

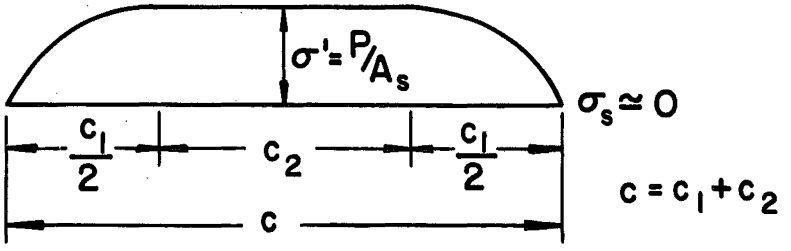

FIG. 2 THE ASSUMED AXIAL STRESS DISTRIBUTION IN THE STEEL AT A CRACKED REGION

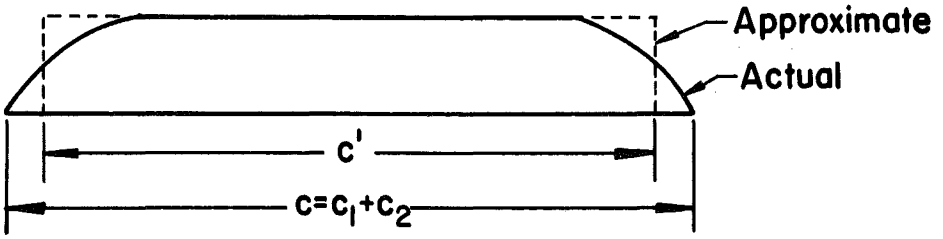

FIG. 3 CONSTANT STRESS DISTRIBUTION FOR THE STEEL

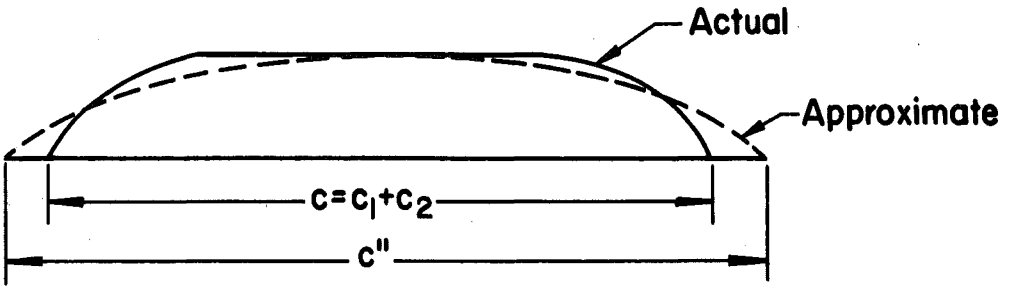

FIG. 4 PARABOLIC STRESS DISTRIBUTION FOR THE STEEL

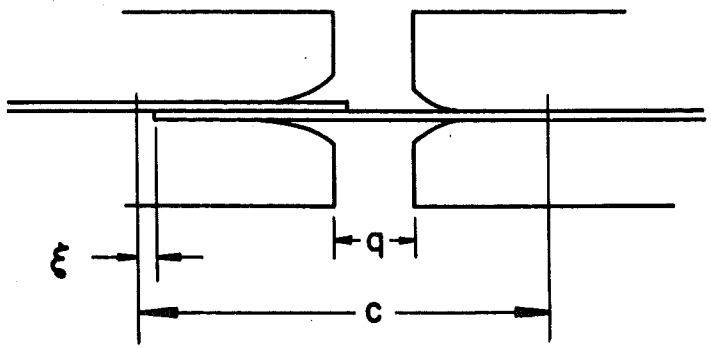

FIG. 5 SLIP AT THE OVERLAP

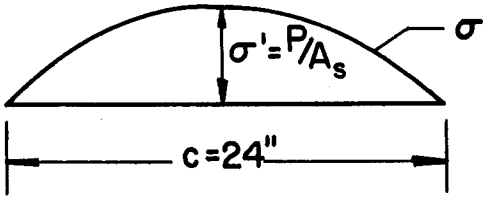

FIG. 6 ASSUMED AXIAL STRESS DISTRIBUTION IN THE STEEL AT OVERLAP

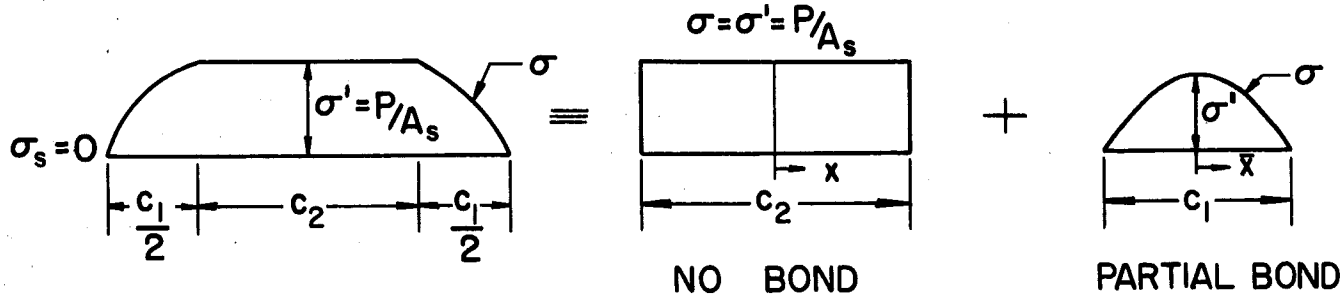

FIG. 7 STEEL STRESSES IN THE UNBONDED AND THE PARTIALLY BONDED SECTIONS NEAR A CRACK

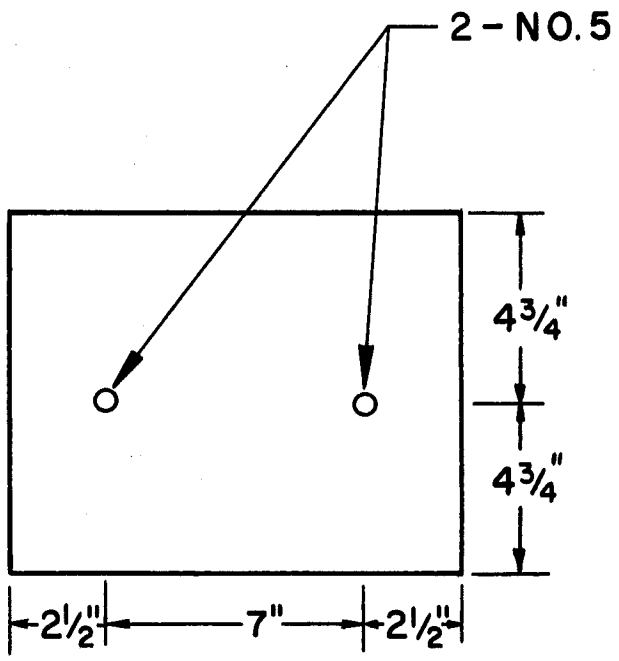

A_c = 114 sq. in.

A_s = 0.62 sq. in.

p = 0.54 %

FIG. 8 CROSS SECTION OF MAIN TEST SPECIMENS

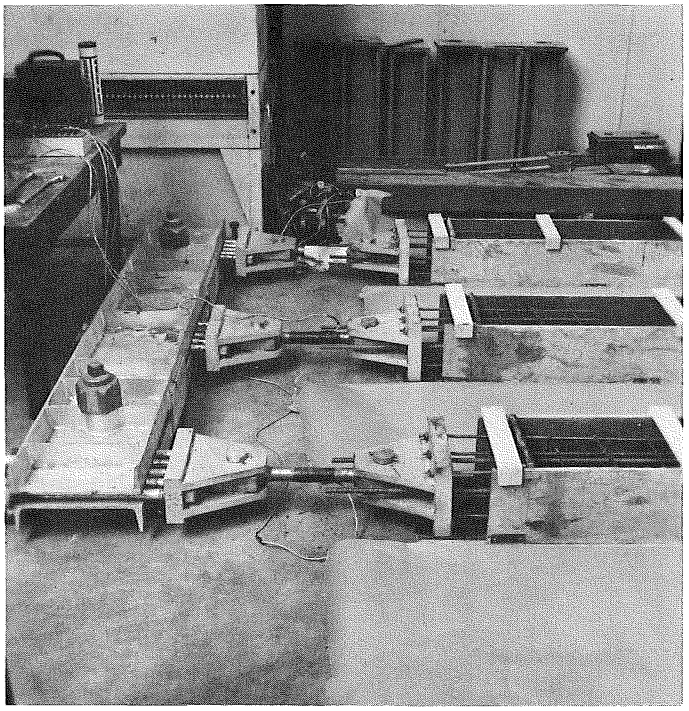

FIG. 9 - FIXED-END OF TEST SPECIMENS

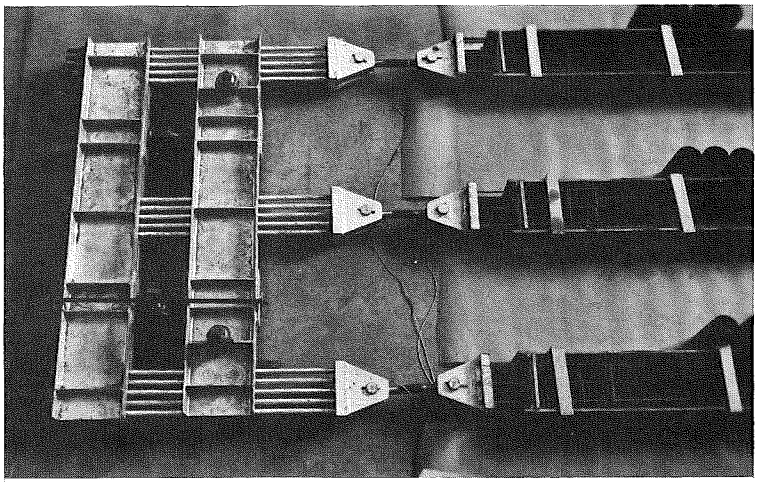

FIG. 10 - MOVING-END OF TEST SPECIMENS

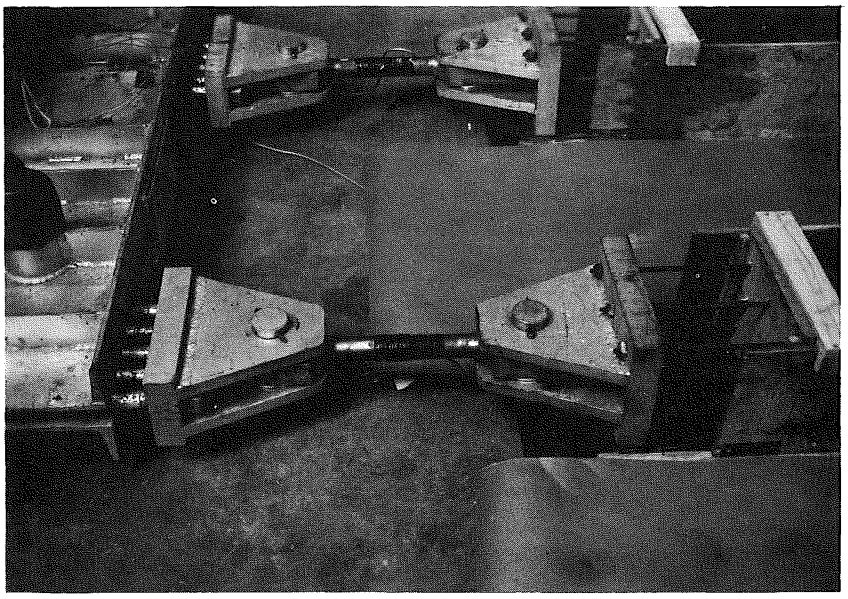

FIG. 11 - DYNAMOMETERS IN PLACE

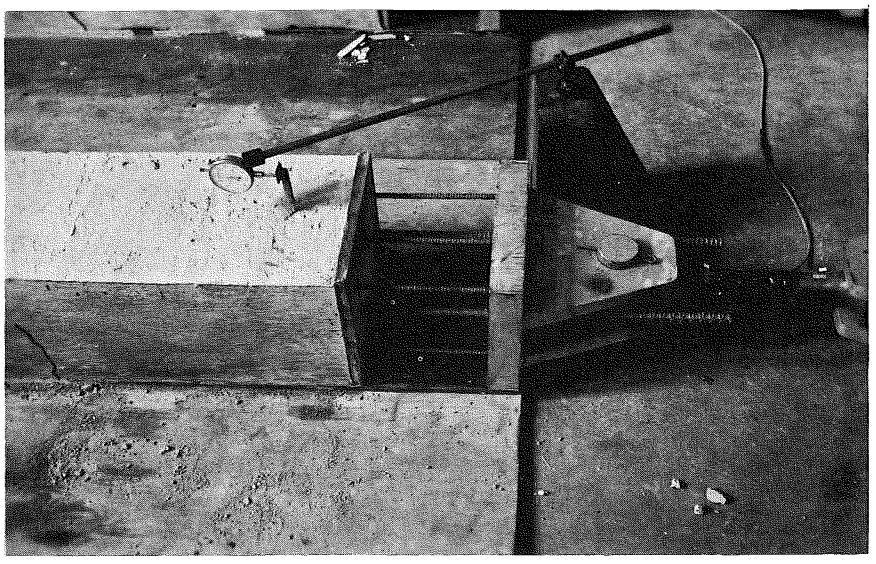

FIG. 12 - END FIXTURE FOR MEASURING TOTAL CHANGE IN LENGTH

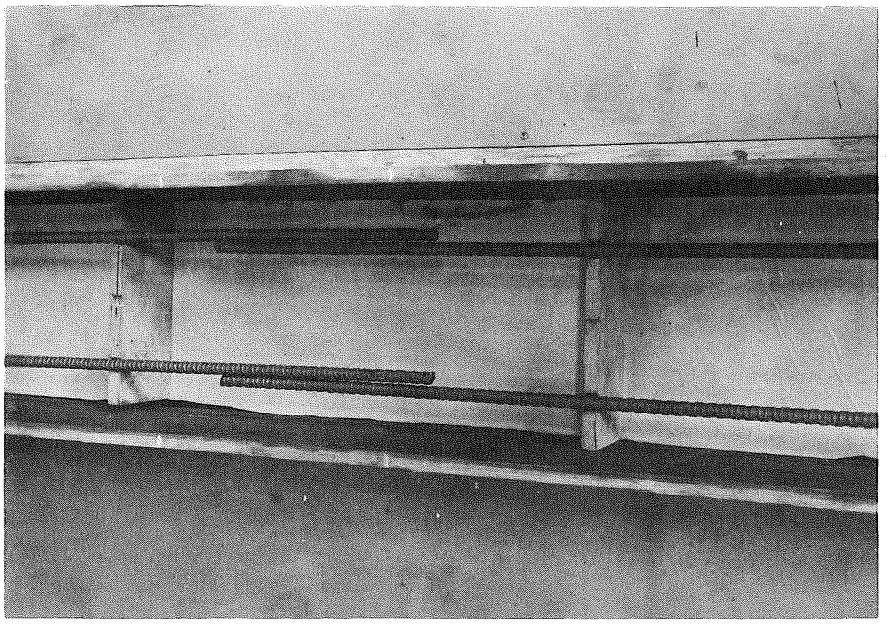

FIG. 13 OVERLAP AT THE MIDDLE SECTION

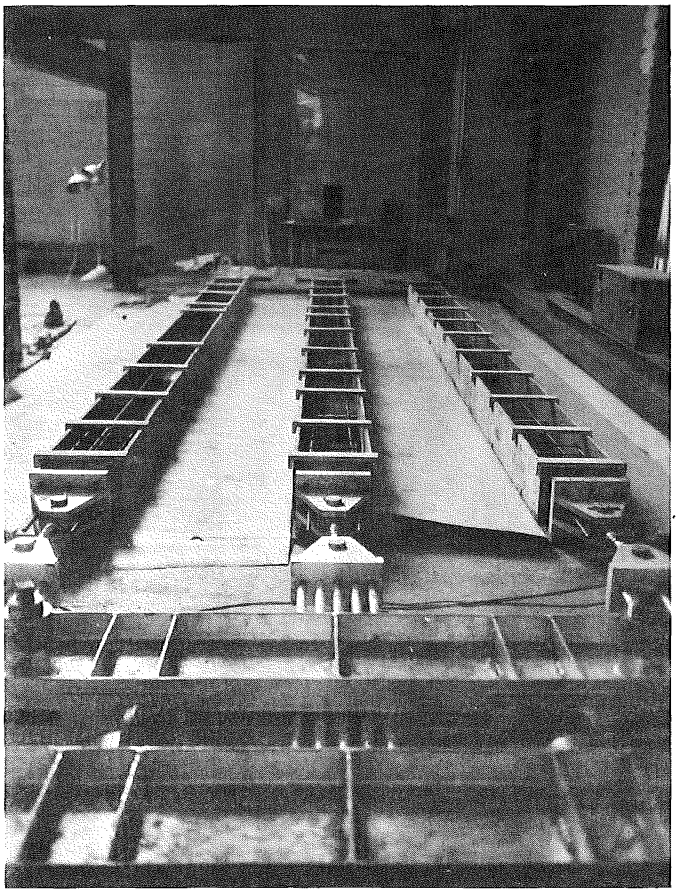

FIG. 14 - GENERAL TEST SET-UP

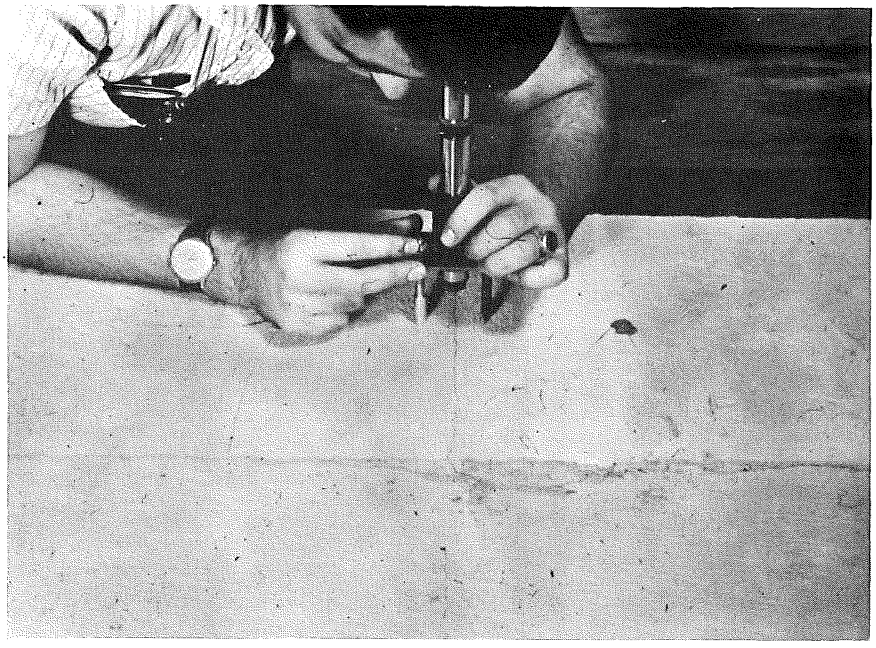

FIG. 15 - CRACK WIDTH MEASUREMENTS WITH OPTICAL DEVICE

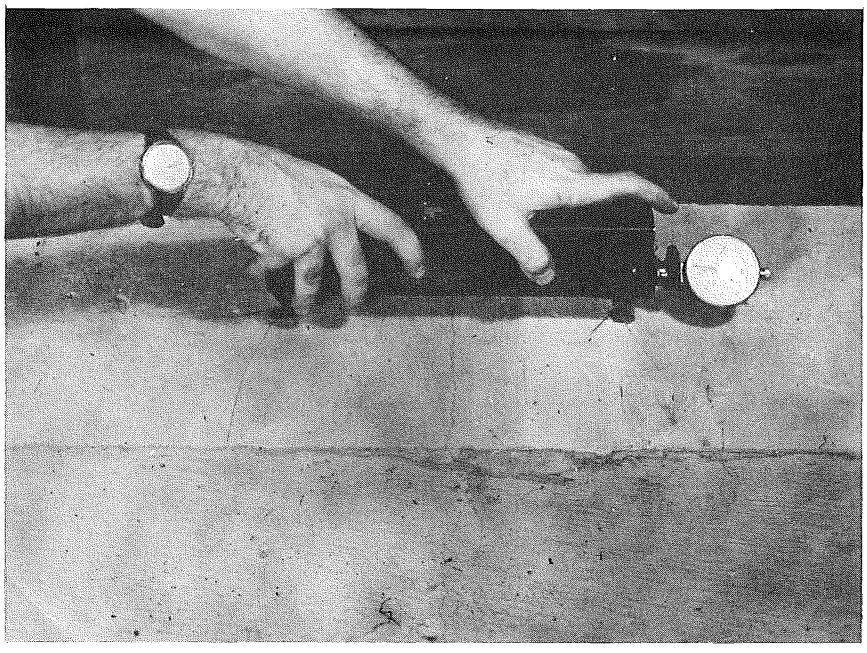

FIG. 16 - CRACK WIDTH MEASUREMENTS WITH WHITTEMORE GAGE

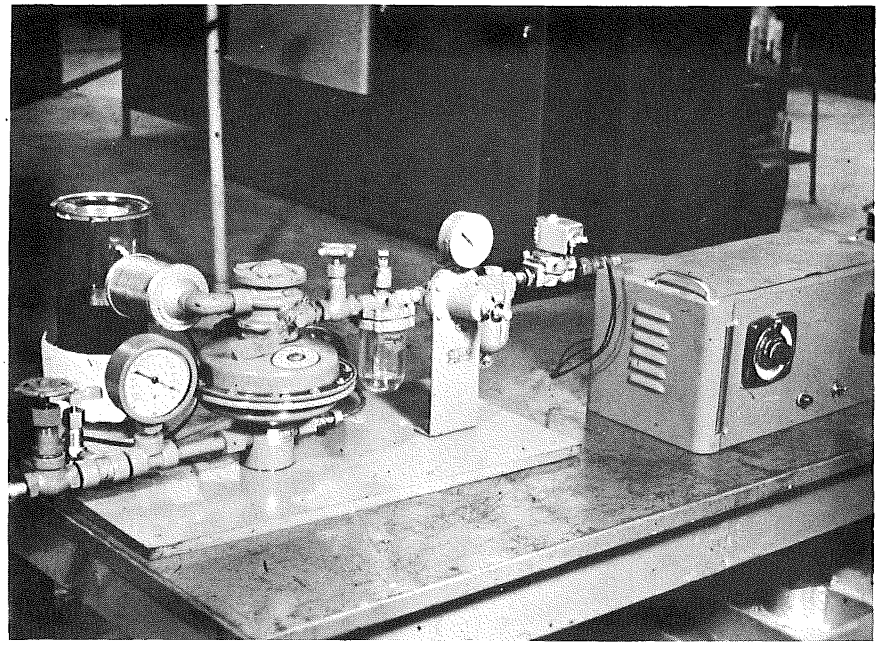

FIG. 17 - TIMER AND LOAD CONTROL UNIT FOR DYNAMIC TESTS

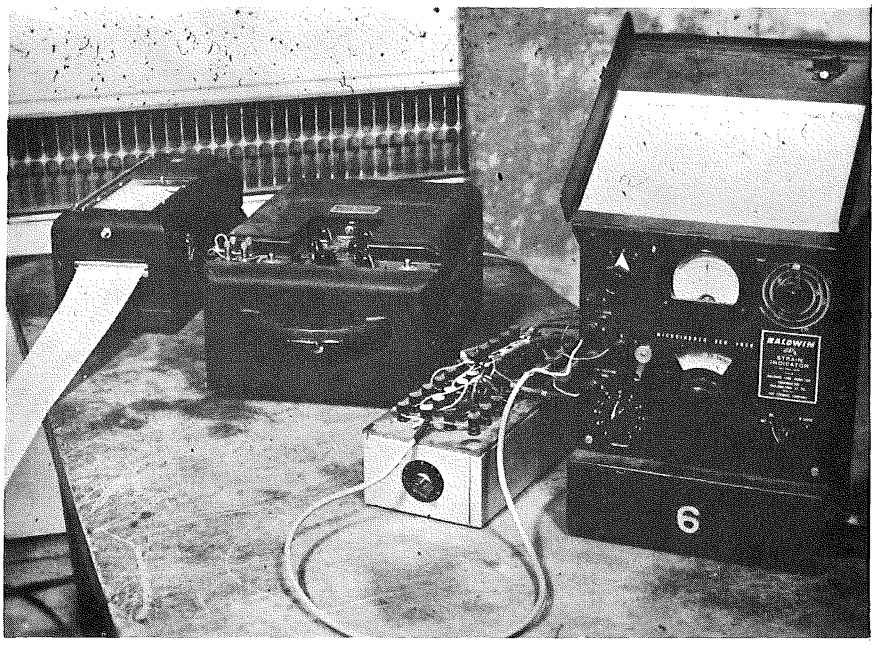

FIG. 18 - STRAIN MEASUREMENTS IN DYNAMIC TESTS
(STRIP CHART RECORDER, AMPLIFIER, STATIC STRAIN INDICATOR)

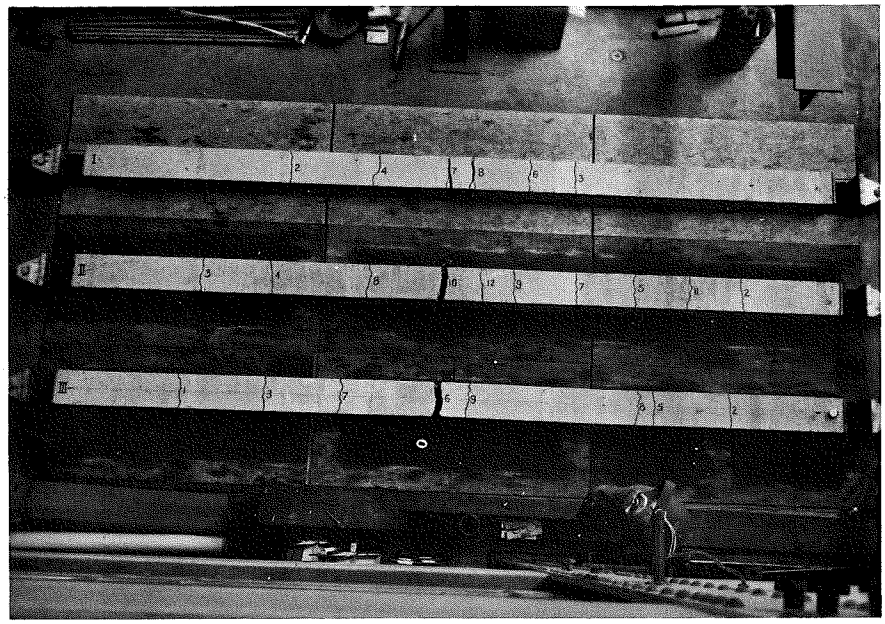

FIG. 19A - CRACK SEQUENCE IN SET A

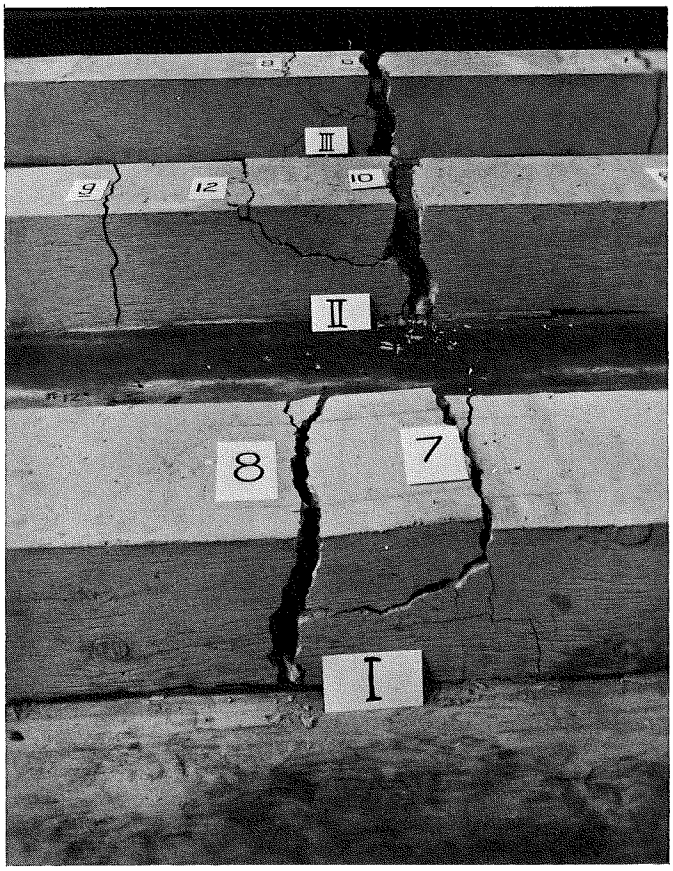

FIG. 19B - FAILURE OF SPECIMENS I,II,III (SET A)

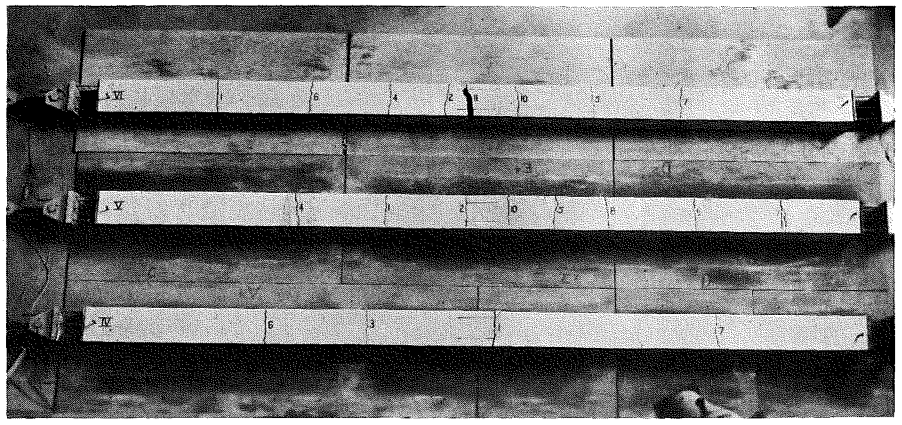

FIG. 20A - CRACK SEQUENCE IN SET B

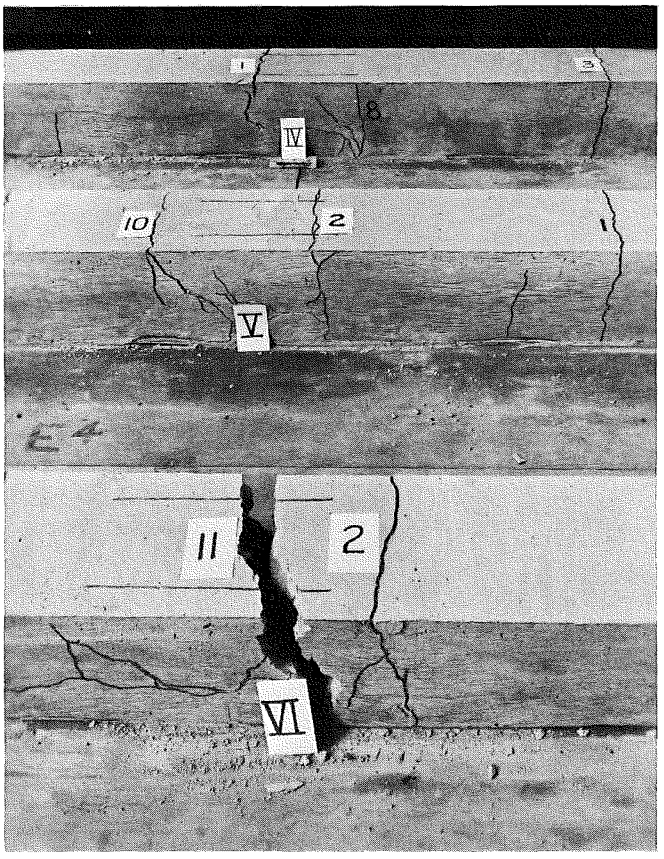

FIG. 20B - FAILURE OF SPECIMENS IV,V,VI (SET B)

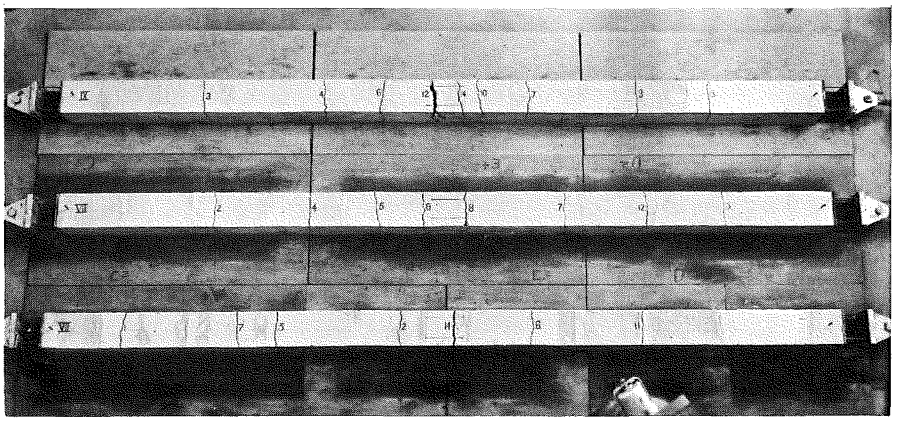

FIG. 21A - CRACK SEQUENCE IN SET C

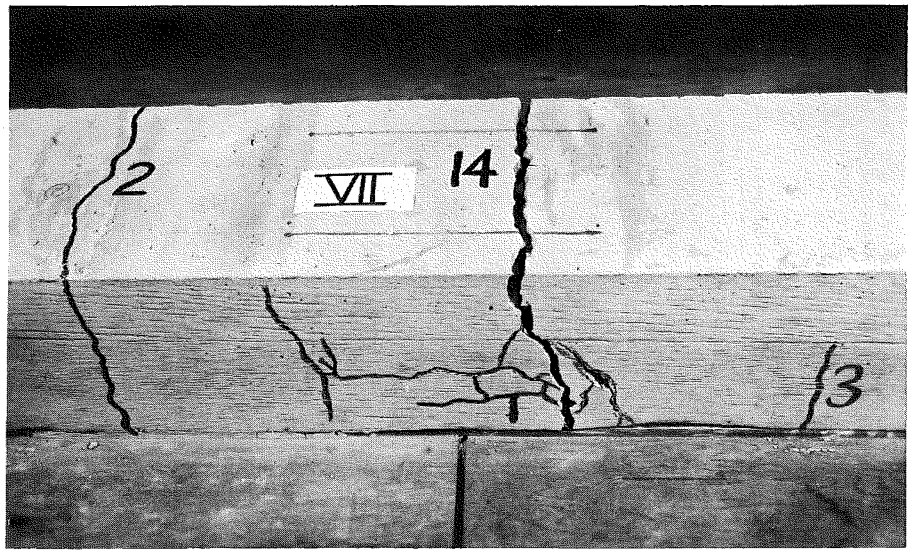

FIG. 21B - FAILURE OF SPECIMEN VII (SET C)

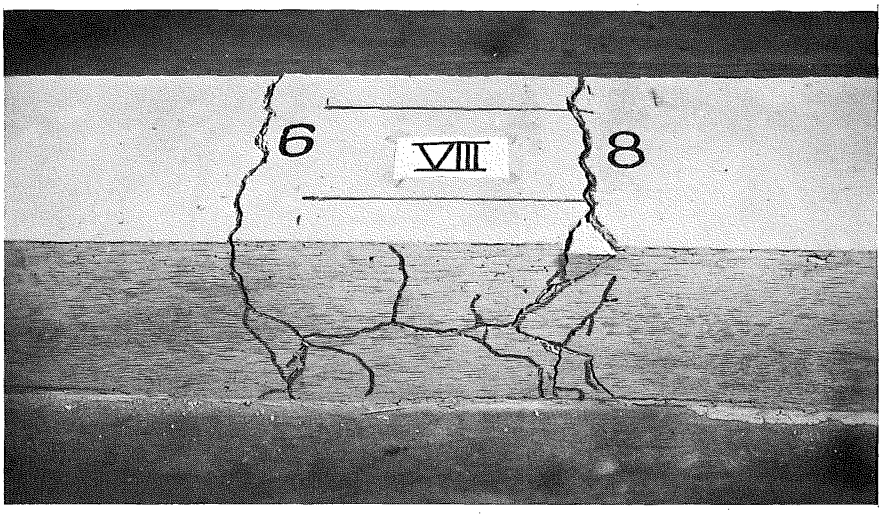

FIG. 21C - FAILURE OF SPECIMEN VIII (SET C)

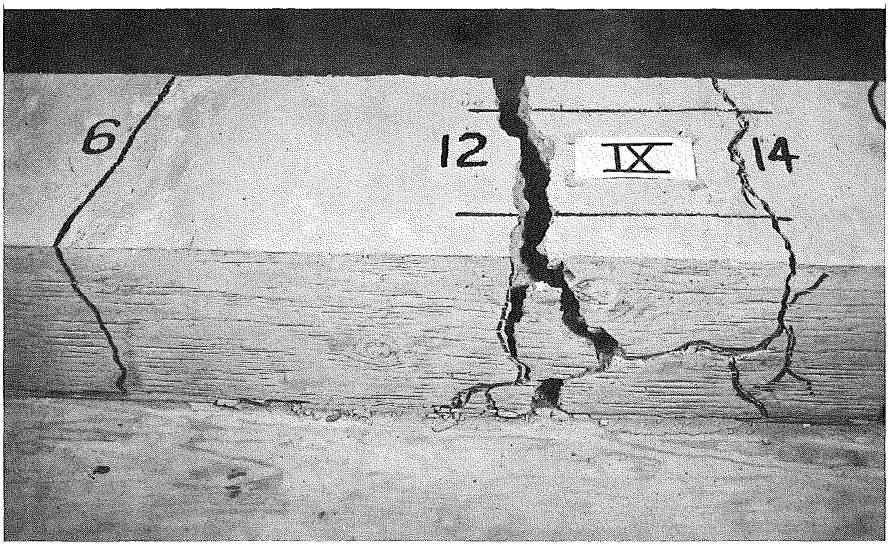

FIG. 21D - FAILURE OF SPECIMEN IX (SET C)

FIG. 22A - CRACK SEQUENCE IN SET D

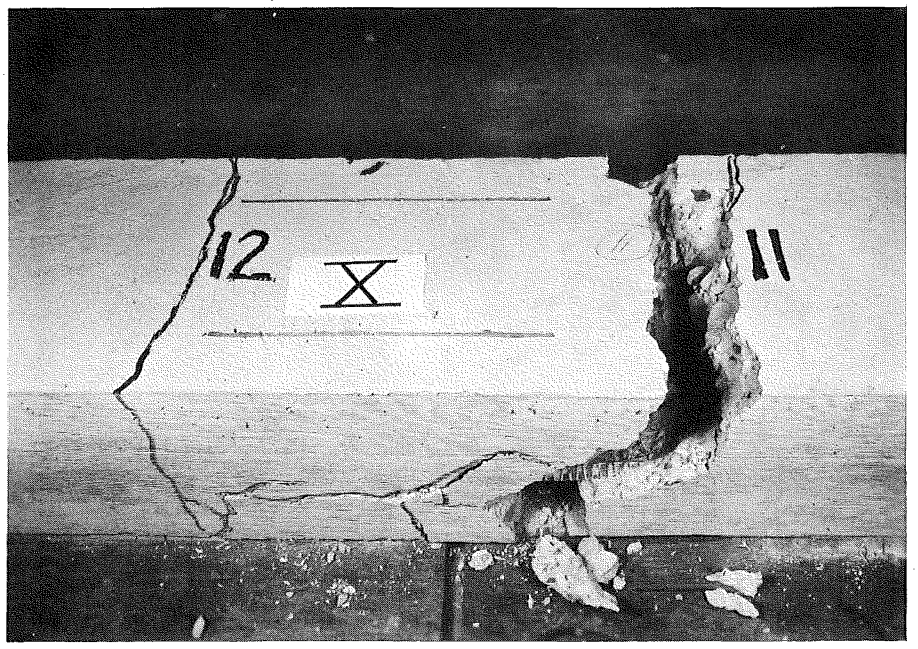

FIG. 22B - FAILURE OF SPECIMEN X (SET D)

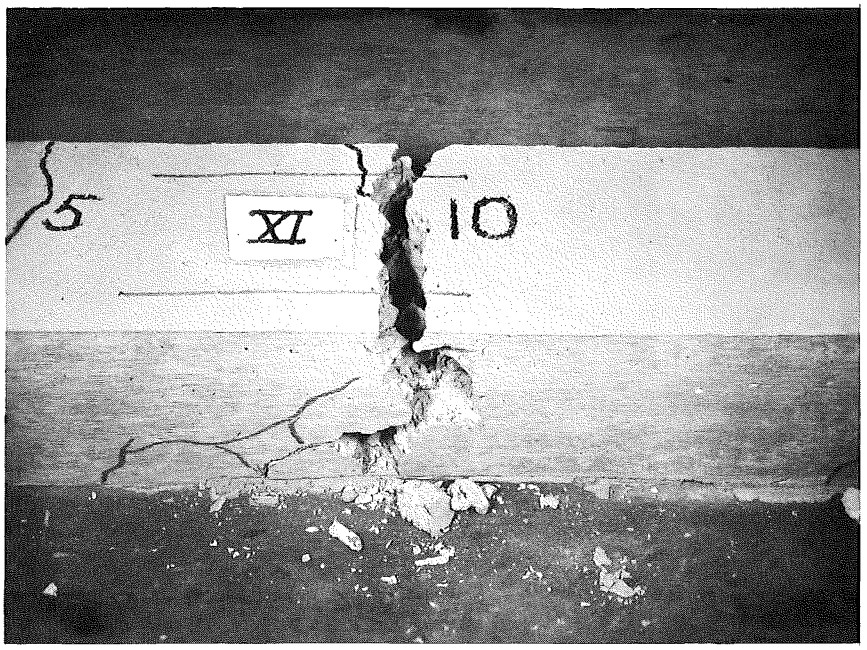

FIG. 22C - FAILURE OF SPECIMEN XI (SET D)

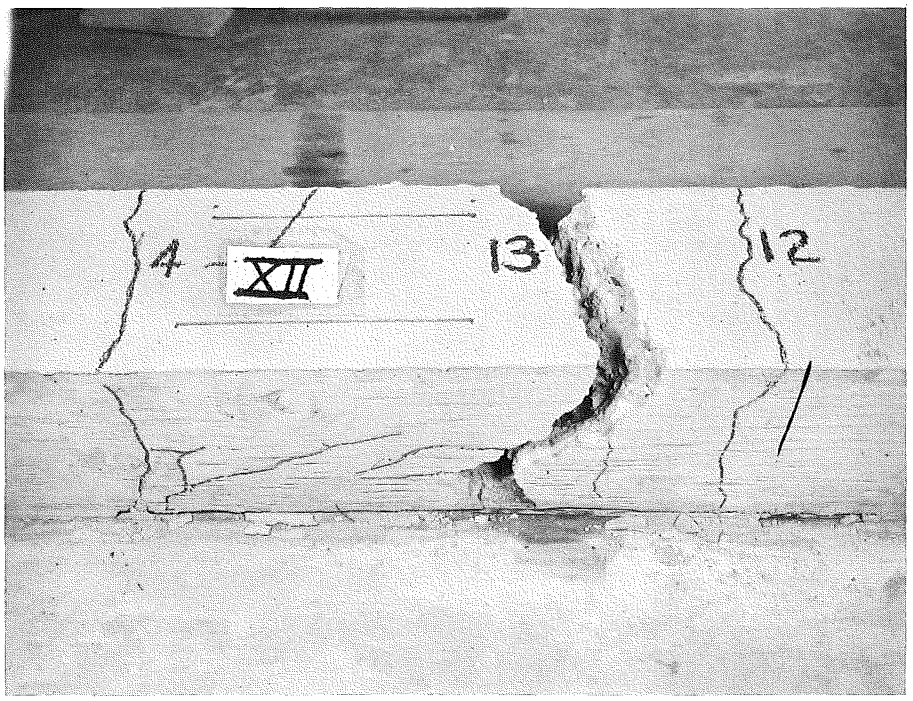

FIG. 22D - FAILURE OF SPECIMEN XII (SET D)

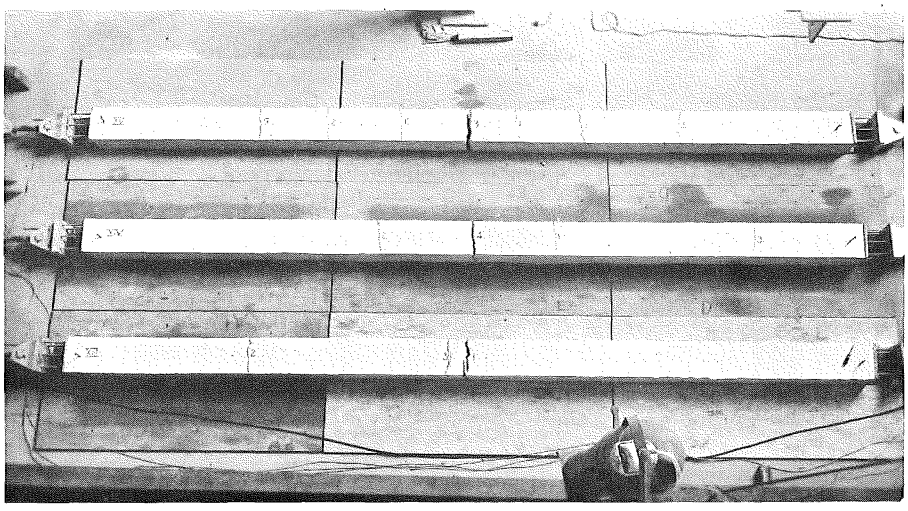

FIG. 23A - CRACK SEQUENCE IN SET E

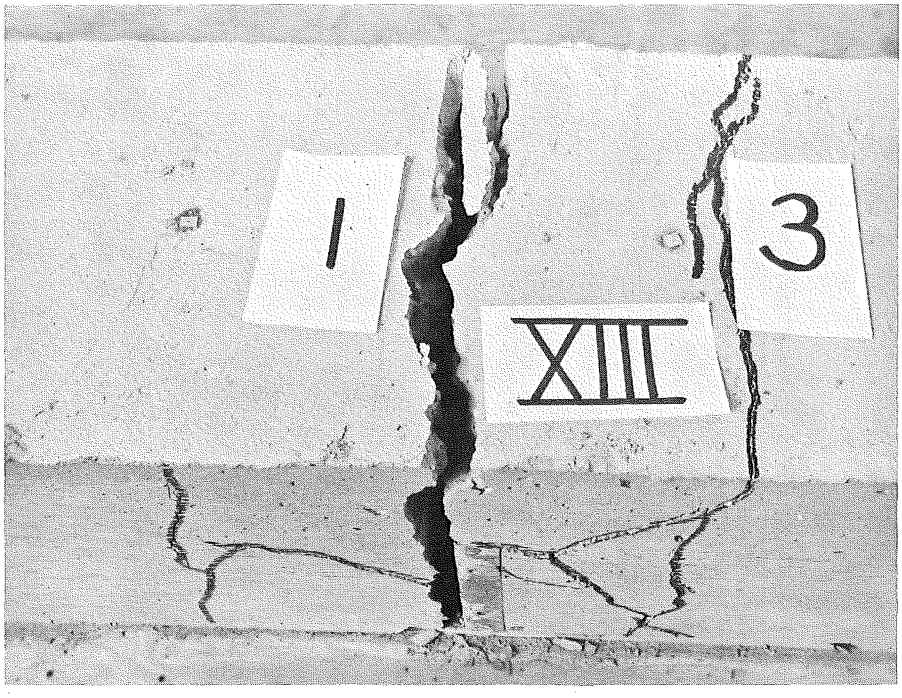

FIG 23B - FAILURE OF SPECIMEN XIII (SET E)

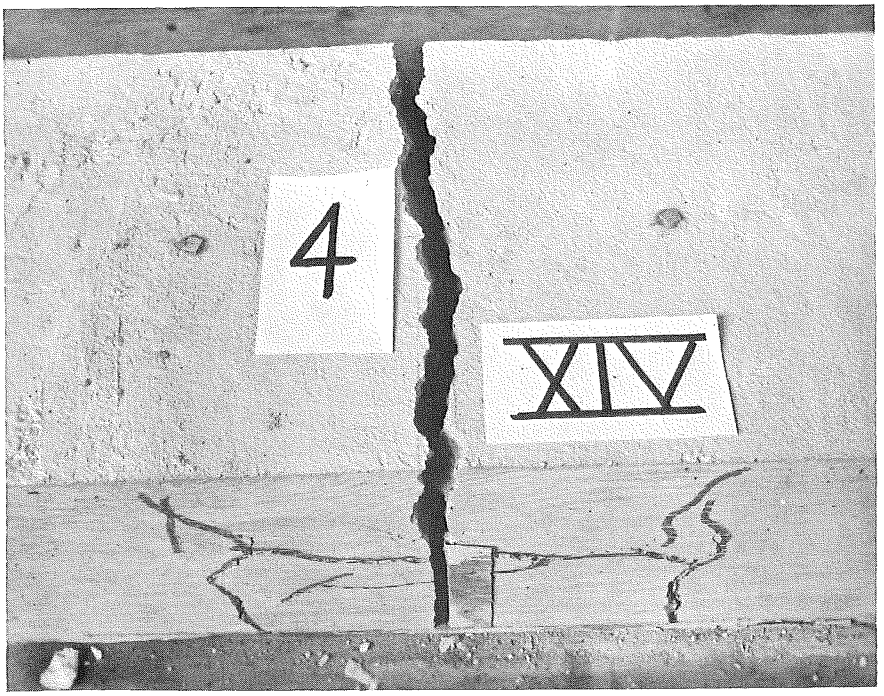

FIG. 23C - FAILURE OF SPECIMEN XIV (SET E)

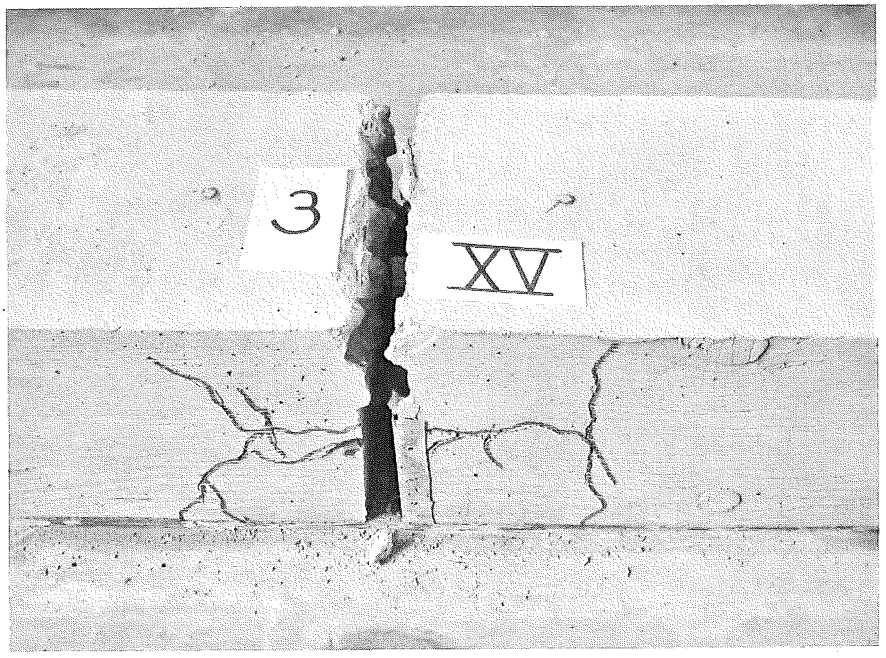

FIG. 23D - FAILURE OF SPECIMEN XV (SET E)

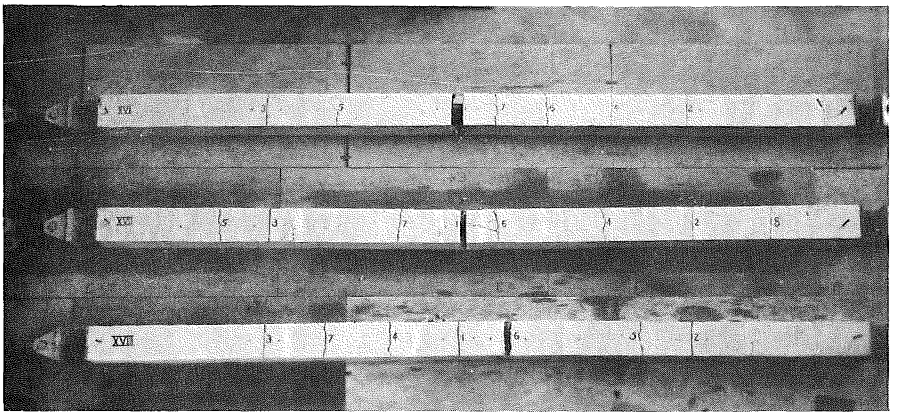

FIG. 24A - CRACK SEQUENCE IN SET F

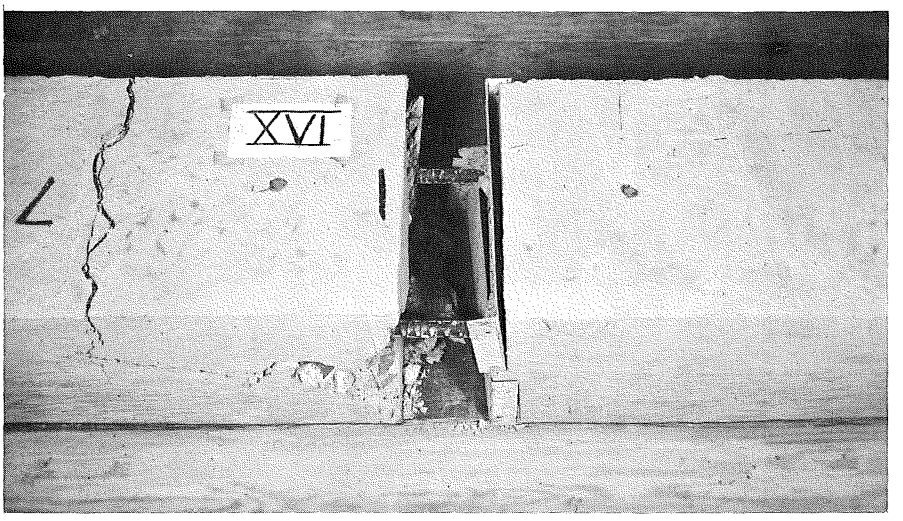

FIG. 24B - FAILURE OF SPECIMEN XVI (SET F)

FIG. 24C - FAILURE OF SPECIMEN XVII (SET F)

FIG. 24D - FAILURE OF SPECIMEN XVIII (SET F)

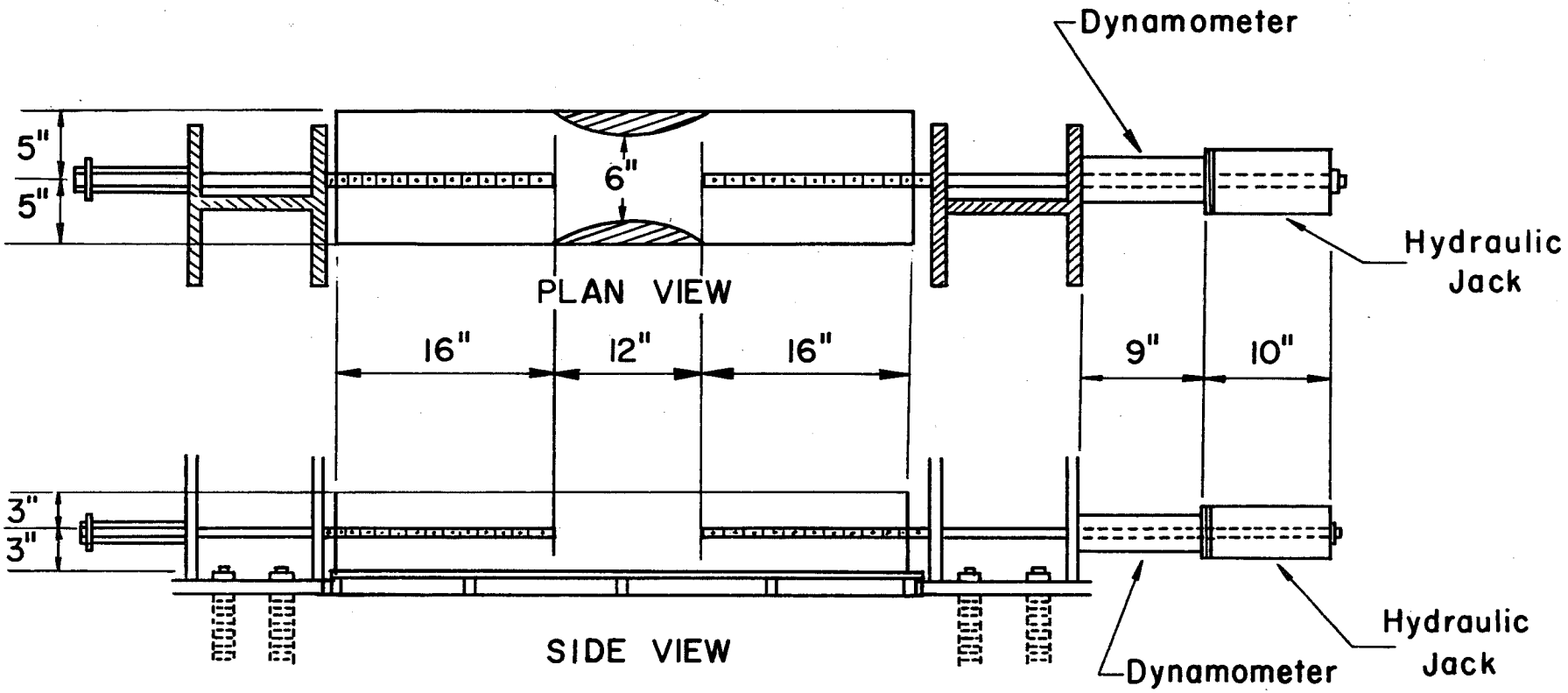

FIG. 25 - TENSION SPECIMENS

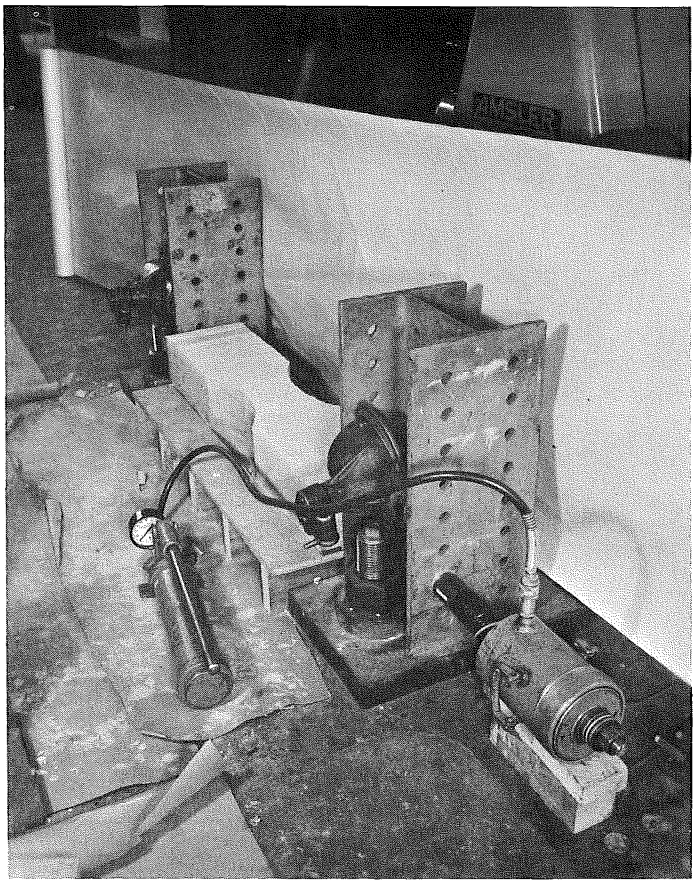

FIG. 26 - TENSION SPECIMEN IN TEST BED

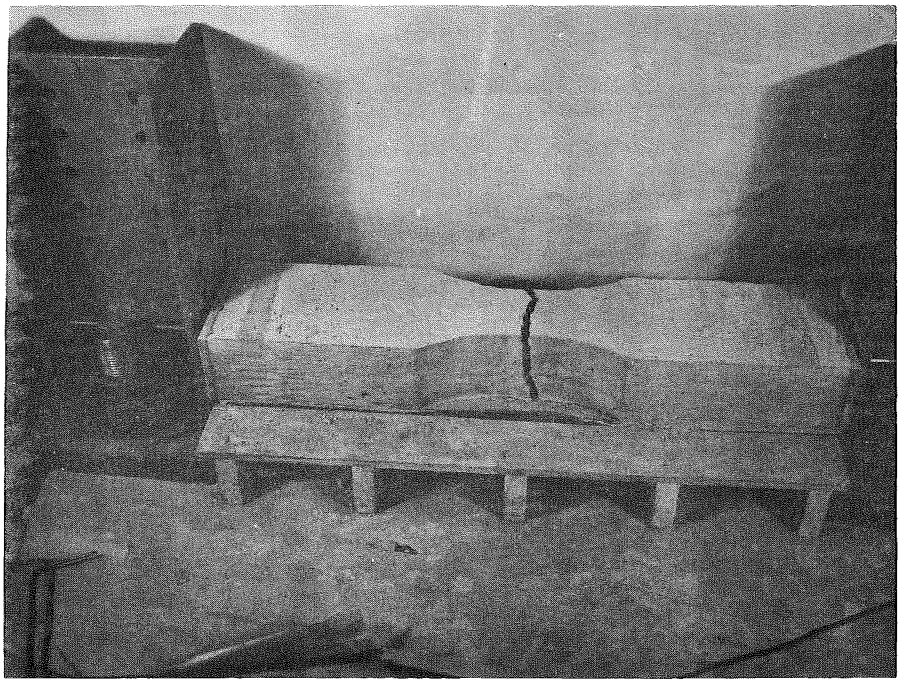

FIG. 27 - TYPICAL FAILURE OF TENSION SPECIMENS

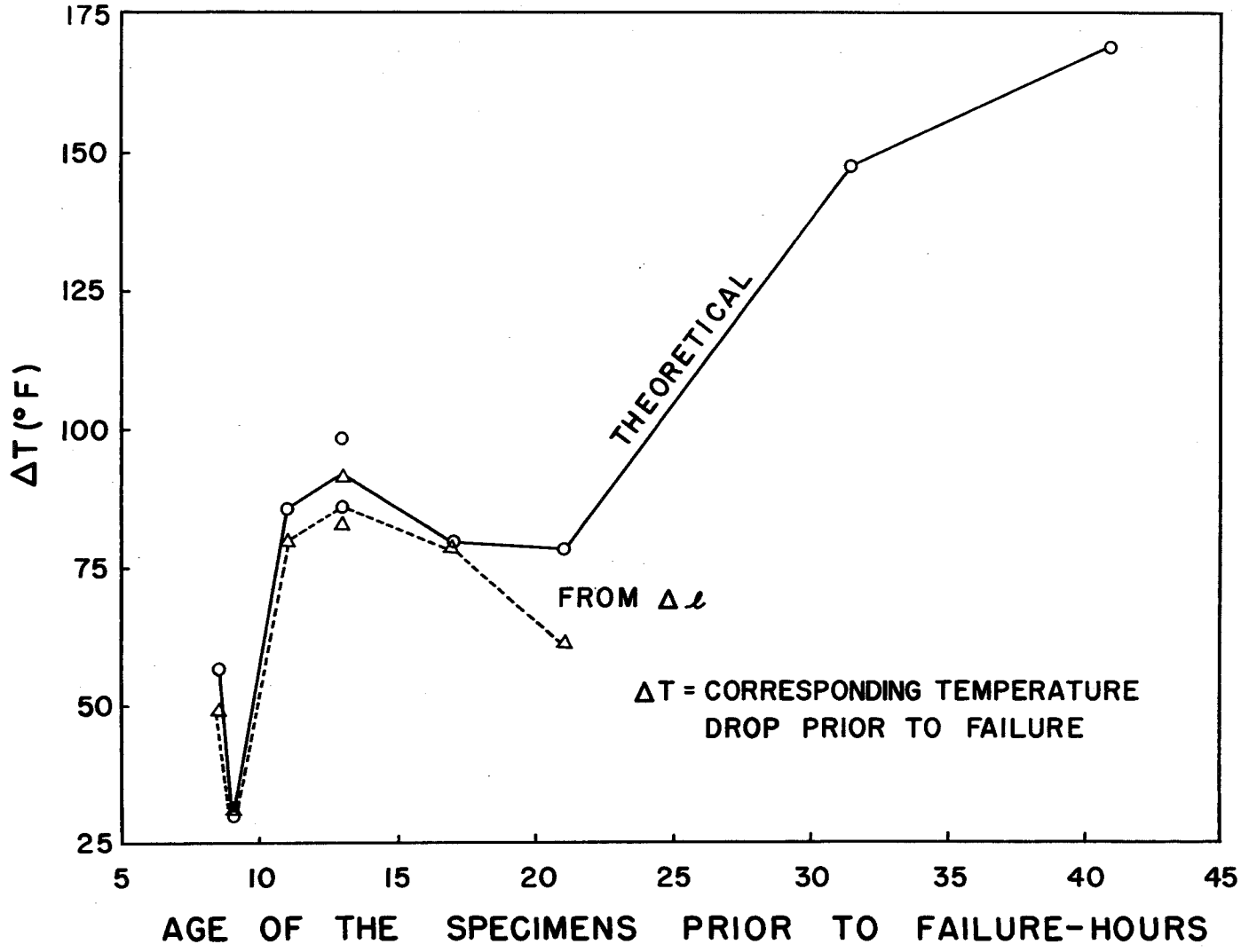

FIG. 28 – ΔT vs. AGE OF THE SPECIMENS FOR STATIC TESTS – SETS A, B, C

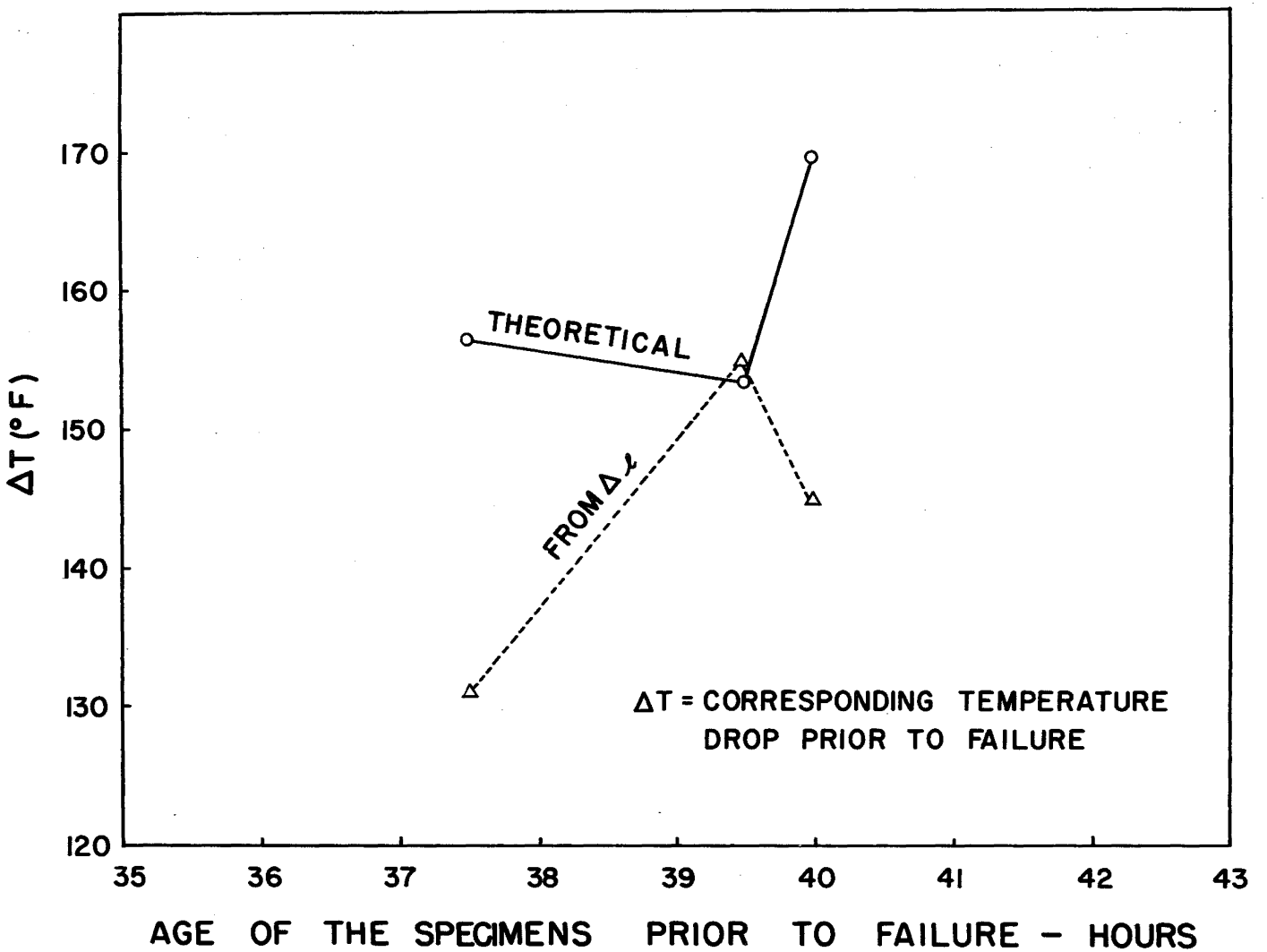

FIG.29 - ΔT vs. AGE PRIOR TO FAILURE FOR SPECIMENS CURED UNDER LOAD-SET D

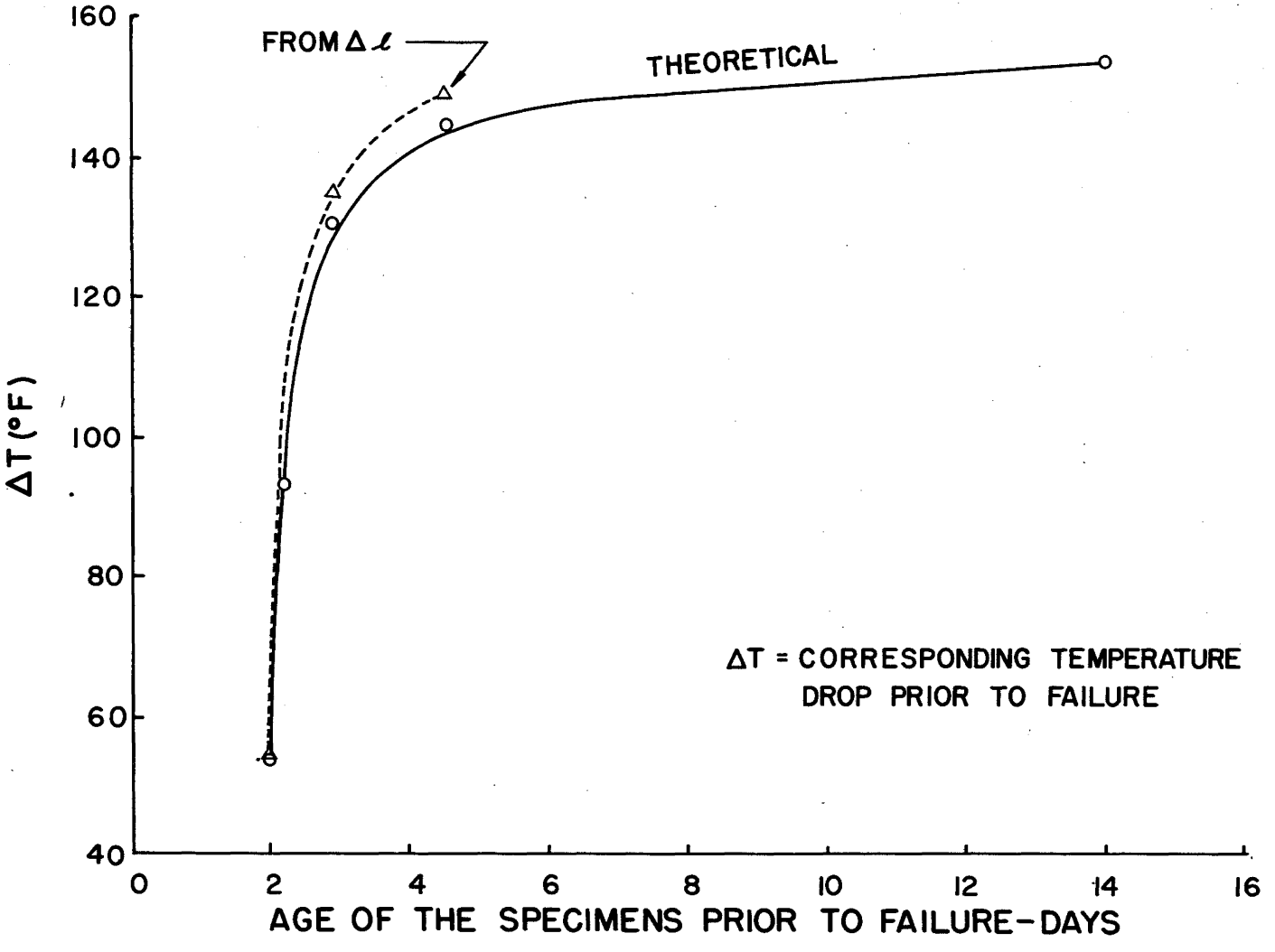

FIG.30 - ΔT vs. AGE OF SPECIMENS PRIOR TO FAILURE FOR DYNAMIC TESTS-SETS E, F

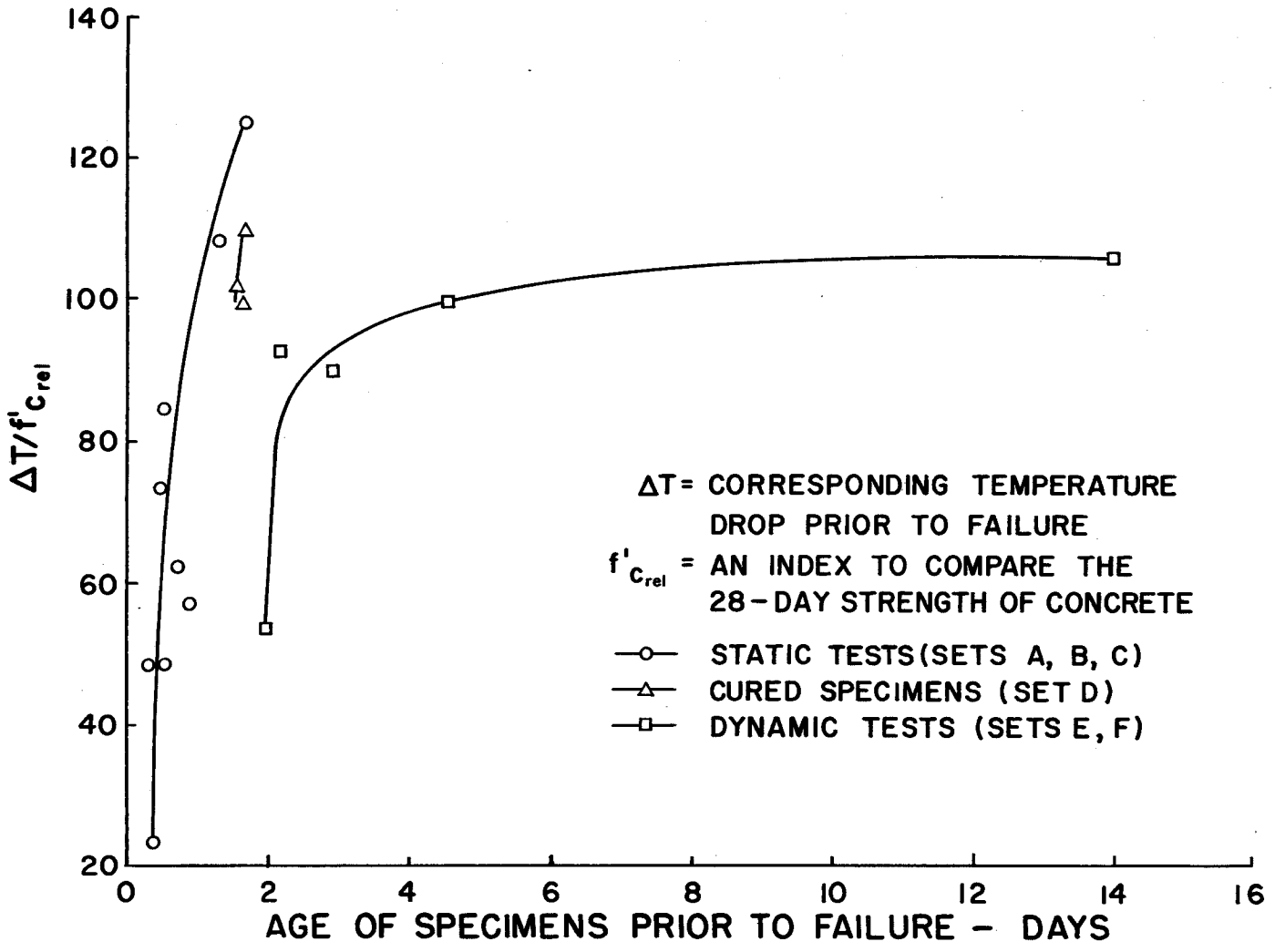

FIG. 31 – $\Delta T/f'_{c_{rel}}$ vs. AGE PRIOR TO FAILURE FOR ALL TESTS

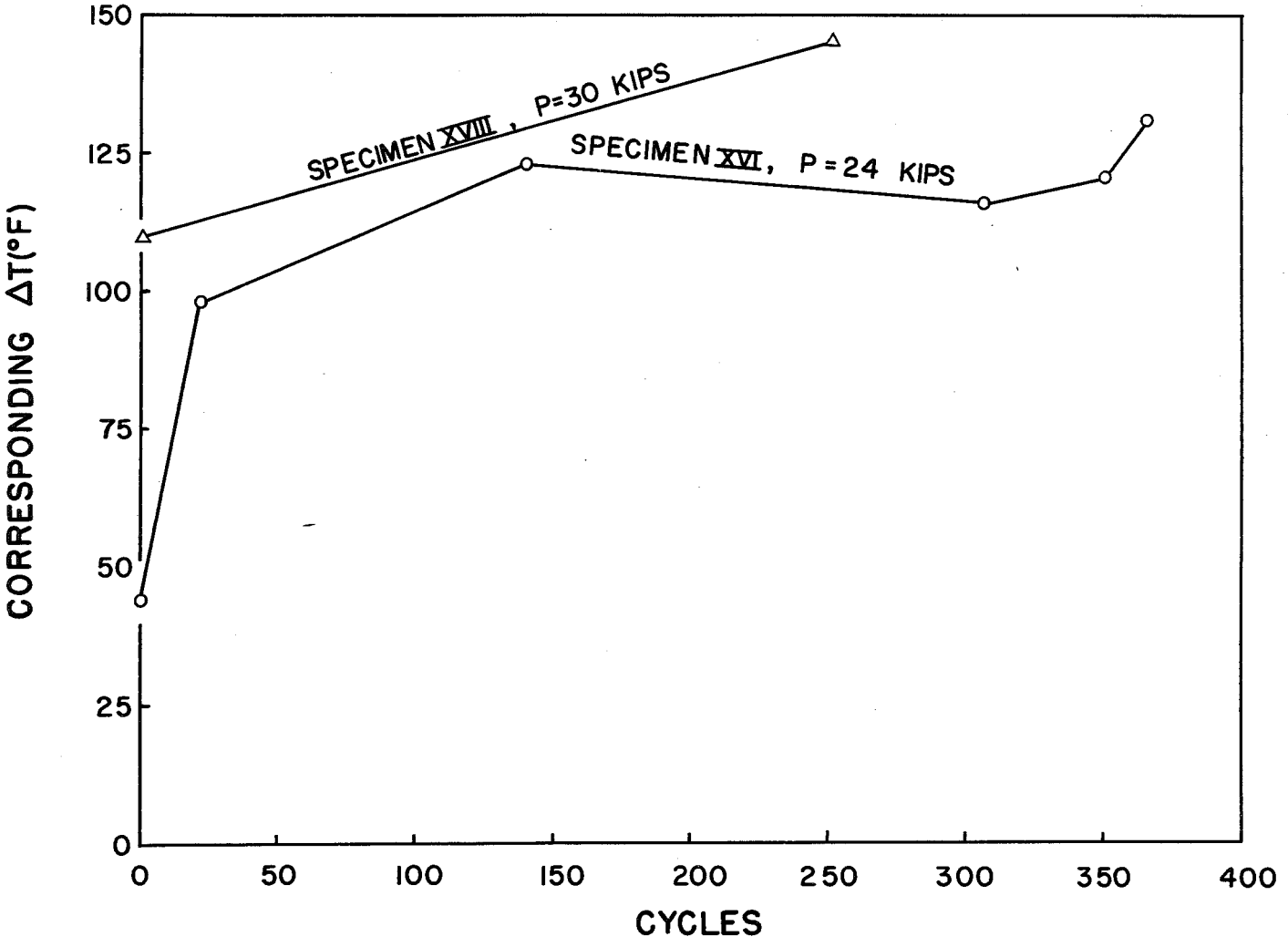

FIG. 32 – EFFECT OF CYCLING ON EQUIVALENT TEMP. CHANGE UNDER CONSTANT AXIAL LOAD

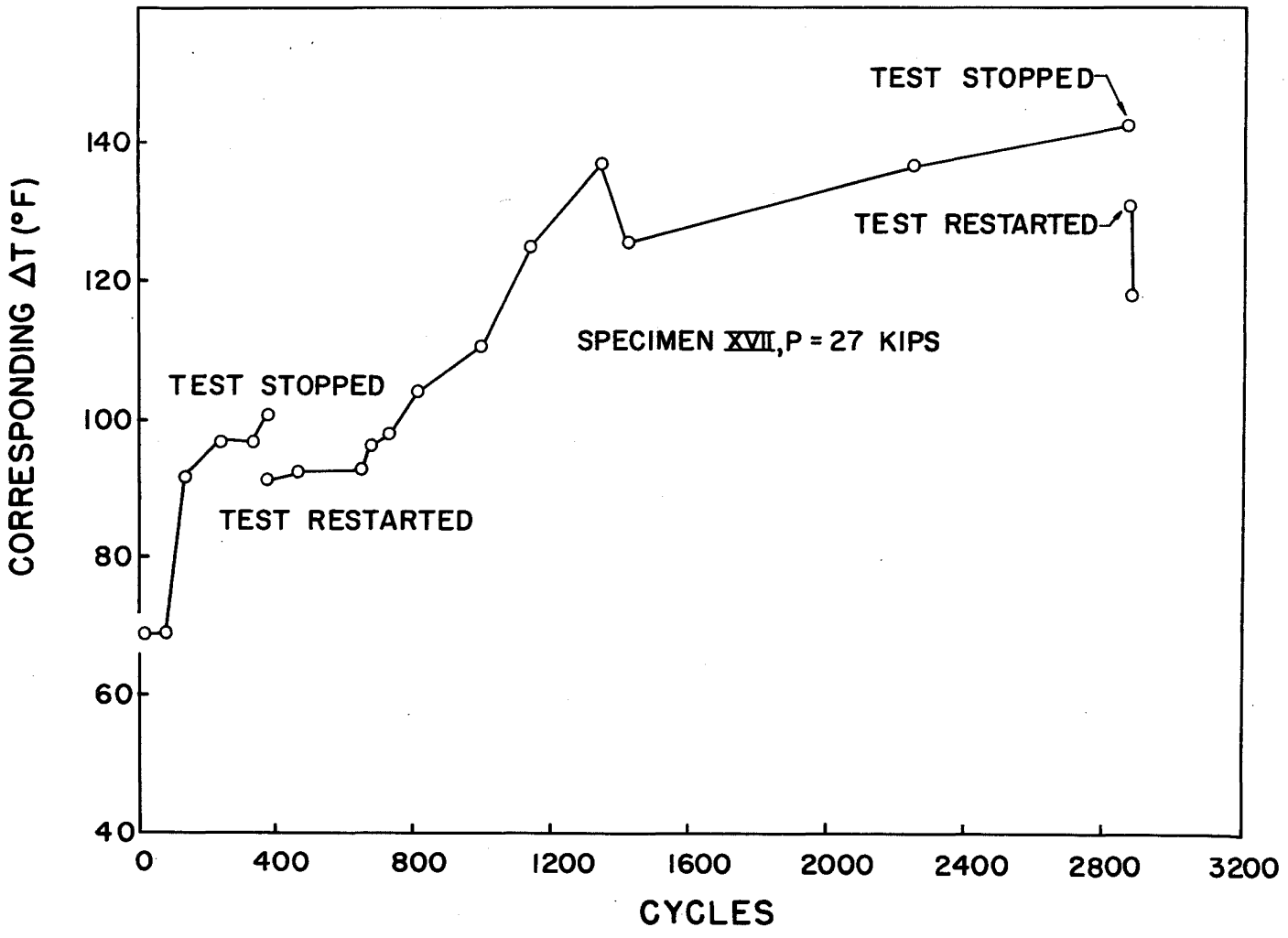

FIG. 33 – EFFECT OF CYCLING ON EQUIVALENT TEMP. CHANGE UNDER CONSTANT AXIAL LOAD

8. REFERENCES

1. Friberg, B.F.
FRICTIONAL RESISTANCE UNDER CONCRETE PAVEMENTS AND RESTRAINT STRESSES IN LONG REINFORCED SLABS
HRB Proc., Vol. 33, 1954, p. 167

2. Gilkey, H.J., Chamberlin, S.J., and Beal, R.W.
BOND BETWEEN CONCRETE AND STEEL AND THE SPACING OF REINFORCEMENT
Iowa State College Eng. Report No. 26

3. Schiffman, R.L.
RESEARCH IN CONTINUOUSLY REINFORCED CONCRETE PAVEMENTS-LITERATURE SURVEY - Fritz Lab. Report 256.1, July 1957

4. Taylor, I.J., Liebig, J.O. Jr., and Eney, W.J.
EXPERIMENTAL PAVEMENT ON US ROUTE 22 IN BERKS COUNTY, PENNSYLVANIA
Fritz Lab. Report 256.9, Sept. 1959

5. Taylor, I.J. and Eney, W.J.
OBSERVATIONS ON THE BEHAVIOR OF CONTINUOUSLY REINFORCED CONCRETE PAVEMENTS IN PENNSYLVANIA
HRB Bulletin 238, p. 22

6. Yerlici, V.A.
AN EXPERIMENTAL STUDY OF THE INFLUENCE OF CONTINUOUS REINFORCEMENT ON THE CRACK PATTERN OF LONG CONCRETE PAVEMENTS
Fritz Lab. Report 256.4, Nov. 1958